[7] Gharib, T. G., Chen, G., Wang, H., Huang, C. C. *et al.*, *Neoplasia* 2002, *4*, 440–448.

[8] Chen, G., Wang, H., Gharib, T. G., Huang, C. C. *et al.*, *Mol. Cell. Proteomics* 2003, *2*, 107–116.

[9] Chen, G., Gharib, T. G., Thomas, D. G., Huang, C. C. *et al.*, *Proteomics* 2003, *3*, 496–504.

[10] Chen, G., Gharib, T. G., Wang, H., Huang, C. C. *et al.*, *Proc. Natl. Acad. Sci. USA* 2003, *11*, 13537–13542.

[11] Cuezva, J. M., Chen, G., Alonso, A. M., Isidoro, A., *et al.*, *Carcinogenesis*, 2005, in press.

[12] Yanagisawa, K., Shyr, Y., Xu, B. J., Massion, P. P., *et al.*, *Lancet* 2003, *362*, 433–439.

[13] Kondo, T., Seike, M., Mori, Y., Fujii, K. *et al.*, *Proteomics* 2003, *3*, 1758–1766.

[14] Shaw, J., Rowlinson, R., Nickson, J., Stone, T., *Proteomics* 2003, *3*, 1181–1195.

[15] Seike, M., Kondo, T., Mori, Y., Gemma, A. *et al.*, *Cancer Res.* 2003, *63*, 4641–4647.

[16] Molina, R., Filella, X., Auge, J. M., Fuentes, R. *et al.*, *Tumour Biol.* 2003, *24*, 209–218.

[17] Virtanen, C., Ishikawa, Y., Honjoh, D., Kimura, M. *et al.*, *Proc. Natl. Acad. Sci. USA* 2002, *99*, 12357–12362.

[18] Seike, M., Kondo, T., Fujii, K., Gemma, A. *et al.*, *Proteomics* 2004, *4*, 2776–2788.

[19] Siegenthaler, G., Hotz, R., Chatellard-Gruaz, D., Didierjean, L. *et al.*, *Biochem. J.* 1994, *302*, 363–371.

[20] Fan, K., Fan, D., Cheng, L. F., Li, C., *Anticancer Res.* 2000, *20*, 4809–4814.

[21] Shi, Y., Han, Y., Wang, X., Zhao, Y. *et al.*, *Gastric Cancer* 2002, *5*, 154–159.

[22] Shi, Y., Zhai, H., Wang, X., Wu, H. *et al.*, *Cell Mol. Life Sci.* 2002, *59*, 1577–1583.

Available online at www.sciencedirect.com
SCIENCE DIRECT®
Journal of Chromatography B, 823 (2005) 82–97
JOURNAL OF CHROMATOGRAPHY B
www.elsevier.com/locate/chromb

Two-dimensional electrophoresis database of fluorescence-labeled proteins of colon cancer cells

Yasuharu Mori [a], Tadashi Kondo [a,*], Tesshi Yamada [a], Akihiko Tsuchida [b], Tetsuya Aoki [b], Setsuo Hirohashi [a]

[a] *Cancer Proteomics Project, National Cancer Center Research Institute, 5-1-1 Tsukiji, Chuo-ku, Tokyo 104-0045, Japan*
[b] *Third Department of Surgery, Tokyo Medical University, Japan*

Received 7 May 2004; accepted 29 May 2005
Available online 11 July 2005

Available online at www.sciencedirect.com
SCIENCE DIRECT®
Journal of Chromatography B, 823 (2005) 82–97
JOURNAL OF CHROMATOGRAPHY B
www.elsevier.com/locate/chromb

Two-dimensional electrophoresis database of fluorescence-labeled proteins of colon cancer cells

Yasuharu Mori [a], Tadashi Kondo [a,*], Tesshi Yamada [a], Akihiko Tsuchida [b], Tetsuya Aoki [b], Setsuo Hirohashi [a]

[a] *Cancer Proteomics Project, National Cancer Center Research Institute, 5-1-1 Tsukiji, Chuo-ku, Tokyo 104-0045, Japan*
[b] *Third Department of Surgery, Tokyo Medical University, Japan*

Received 7 May 2004; accepted 29 May 2005
Available online 11 July 2005

Abstract

We constructed a novel database of the proteome of DLD-1 colon cancer cells by two-dimensional polyacrylamide gel electrophoresis (2D-PAGE) of fluorescence-labeled proteins followed by matrix-assisted laser desorption/ionization time-of-flight mass spectrometry (MALDI-TOF) analysis. The database consists of 258 functionally categorized proteins corresponding to 314 protein spots. The majority of the proteins are oxidoreductases, cytoskeletal proteins and nucleic acid binding proteins. Phosphatase treatment showed that 28% of the protein spots on the gel are phosphorylated, and mass spectrometric analysis identified 21 of them. Proteins of DLD-1 cells and of laser-microdissected colon cancer tissues showed similar distribution on 2D gels, suggesting the utility of our database for clinical proteomics.

Keywords: Proteome; Two-dimensional gel electrophoresis; 2D database; 2D-DIGE; colon cancer

1. Introduction

Two-dimensional polyacrylamide gel electrophoresis (2D-PAGE) is an established method of protein separation [1,2], and has been used in many types of biological studies to monitor protein expression in a global manner [3,4]. However, analysis by 2D-PAGE is hampered by low reproducibility due to electrophoretic artifacts and by the limited dynamic range of spot intensity. Recently, novel fluorescent dyes have been developed and used for fluorescence two-dimensional difference gel electrophoresis (2D-DIGE) (Amersham Biosciences, Buckinghamshire, UK) with the aim of solving the problems inherent to 2D-PAGE. In 2D-DIGE, multiple samples are differentially labeled with different fluorescent dyes, mixed together, and co-separated in the same gel. Multiple 2D images are obtained by scanning the gel with appropriate wavelengths specific for each fluorescent dye [5–8]. Because samples are run concomitantly in the same gel, artifactual differences produced by electrophoresis can be distinguished from biological alterations, and spot matching can be performed in a less labor-intensive manner. 2D-DIGE also allows more accurate quantitative analysis of protein expression, since, by their nature, fluorescent dyes have a broader and more quantitative dynamic range than do colorimetric-based staining systems. In addition, the replacement of labor-intensive staining procedures by a simple laser scan enables high-throughput spot detection. With these advantages, 2D-DIGE has been applied to the study of breast cancer [9], esophageal cancer [10], and colon cancer [11]. However, global identification of the proteins corresponding to protein spots has been performed only on 2D images visualized by colorimetric methods, including

Abbreviations: 2D-PAGE, two-dimensional polyacrylamide gel electrophoresis; 2D-DIGE, fluorescence two-dimensional difference gel electrophoresis; MALDI-TOF, matrix-assisted laser desorption/ionization time-of-flight mass spectrometry; CIAP, calf intestine alkaline phosphatase; IPG, immobilized pH gradient; DHB, dihydroxybenzoic acid; DTT, dithiothreitol; TPCK, *N*-tosyl-L-phenylalanine chloromethyl ketone

* Corresponding author. Tel.: +81 3 3542 2511; fax: +81 3 3547 5298.
E-mail address: takondo@gan2.res.ncc.go.jp (T. Kondo).

1570-0232/$ – see front matter © 2005 Elsevier B.V. All rights reserved.
doi:10.1016/j.jchromb.2005.05.024

silver staining [12], SYPRO Ruby [13] and Coomassie Brilliant Blue [14]. Because 2D databases have been created using only these images, the potential of 2D-DIGE for differential expression analysis has not been fully explored.

In this study, we studied the 2D image of fluorescence-labeled proteins. We identified by mass spectrometry (MS) 258 proteins corresponding to 314 fluorescence-labeled protein spots and functionally grouped the identified proteins according to the Panther Category classification in the Celera Discovery System. We discuss the characteristics of the proteins observed by 2D-DIGE, and the possible application of this technology for cancer research.

2. Materials and methods

2.1. Materials

1-(5-Carboxypentyl)-1′-propylindocarbocyanine halide *N*-hydroxy-succinimidyl ester (Cy3 fluorescent dye), 1-(5-carboxypentyl)-1′-methylindodi-carbocyanine halide *N*-hydroxysuccinimidyl ester (Cy5 fluorescent dye), and Decyder software Version 4.0 were purchased from Amersham Biosciences (Little Chalfont, Buckinghamshire, UK).

2.2. Cell culture, clinical material, and protein extraction

The human colon cancer cell line DLD-1 was obtained from the American Type Culture Collection (ATCC; Rockville, MD) and maintained in a humidified CO_2 incubator with RPMI-1640 medium supplemented with 10% FBS. DLD-1 cell protein samples were prepared as follows. After washing the cells with PBS and incubating them with 10% trichloroacetic acid (TCA) for 30 min on ice, they were scraped off and collected by brief centrifugation. The cell pellet was then suspended with lysis buffer (6 M urea, 2 M thiourea, 3% CHAPS and 1% Triton X-100) for 30 min on ice. The protein sample was centrifuged at 15,000 rpm for 30 min at 4 °C, and the supernatant was recovered.

Colon cancer tissue was obtained from a surgical specimen from a patient with colon cancer at Tokyo Medical University after obtaining the patient's informed consent. Laser microdissection was performed as described previously [15]. Briefly, the surgically resected colon cancer tissue was snap-frozen in liquid nitrogen immediately after resection and embedded in optimal cutting temperature (O.C.T.) compound (Sakura Finetechnical Co., Ltd., Tokyo, Japan). The O.C.T. embedded tissue blocks were cut into 10 μm thick sections with a Leica cryostat CM 3050 S (Leica, Milton Keynes, UK). The sectioned tissues were placed on a membrane-coated slide glass (Leica) pretreated with tissue adhesive solution, 0.1% poly-L-lysine (Sigma, St. Louis, MO). The sectioned tissues were fixed with 95% ethanol for 30 s [DD1] and washed in water. After being soaked in Mayer's hematoxylin (Muto Pure Chemicals, Tokyo, Japan) for 1 min, they were washed twice in 95% ethanol and once in water, each for 10 s. The neighboring section was occasionally stained with standard hematoxyline and eosine to confirm the diagnosis. All staining procedures were carried out on ice. Under microscopic observation, colon cancer cells were isolated with the Leica Microdissection System (Leica). The isolated tumor cells were treated with lysis buffer as described above.

Protein concentration was measured with a Protein Assay Kit (Bio-Rad Laboratories, Inc., Hercules, CA) and adjusted to 1 mg/ml with lysis buffer. The pH of the samples was adjusted to 8.5 with 30 mM Tris–HCl, a 50 μg protein sample was labeled with Cy3 or Cy5 fluorescent dye for 30 min, and the labeling reaction was terminated by adding 0.2 mM lysine for 10 min. The labeled sample was then incubated for 15 min with an equal volume of lysis buffer containing 130 mM DTT and 2.0% ampholine (Amersham Biosciences), and the total volume of the sample was adjusted to 420 μl with lysis buffer containing 65 mM DTT and 1.0% ampholine. All procedures after the start of the labeling reaction were carried out on ice in the dark.

2.3. 2D-PAGE

2D-PAGE was performed as described previously [1]. Briefly, IPG strip gels (24 cm long, p*I* range 3.0 and 10.0; Amersham Biosciences) were allowed to rehydrate with a labeled protein sample for 12 h at 20 °C. Isoelectric focusing was carried out with an IPGphor (Amersham Biosciences) for a total of 80 kVh at 20 °C. The IPG gel was equilibrated with equilibration buffer containing 3 M urea, 50 mM Tris–HCl (pH 8.8), 30% glycerol, 1.0% SDS, and 16 mM DTT for 15 min with gentle agitation. Another incubation was then carried out with the equilibration buffer in which DTT was replaced by 122 mM iodoacetamide. A 9–15% gradient polyacrylamide gel between low-fluorescence glass plates measuring 200 mm × 240 mm × 1 mm was used in the second separation. The equilibrated IPG gel was placed on the top of the second-dimension gel with embedding agarose (Amersham Biosciences), and the second-dimension electrophoresis was performed at 20 °C for 15 h at 18 W per gel with the EttanDalt II system (Amersham Biosciences). For preparative purposes, we applied 550 μg of protein sample. Although several hundreds of protein samples were required for preparative purpose, it is very costly to label whole proteins with fluprescent dyes. Because labeled and unlabeled proteins had almost identical electrophoretic mobility and 50 μg protein was enough for spot detection, we mixed 500 μg of unlabeled protein sample with 50 μg of labeled protein and separated them together in the same gel for preparative purpose. The second-dimension separation was performed as described above, except that the concentration of DTT was increased to 162 mM for the first equilibration, and iodoacetamide was replaced by 0.05% acrylamide for the second equilibration. The second-dimension gel was bonded to the inner plate

coated with bind-silane solution (Amersham Biosciences) according to the manufacturer's protocol. All electrophoresis procedures were performed in the dark.

2.4. Gel imaging and spot collection

The gels containing fluorescence-labeled proteins were scanned directly between the glass plates with a laser scanner (2D Master Gel Imager; Amersham Biosciences). After scanning, the same gel was stained with SYPRO Ruby dye (Molecular Probes, Eugene, OR) as follows. Briefly, the gel was fixed in 30% (v/v) methanol and 7.5% (v/v) acetic acid for 1 h, and after being washed with water it was incubated with SYPRO Ruby for 3 h at room temperature. The gel image was then read with a 2D Master Gel Imager. The images were exported to the DeCyder software as 16-bit tiff files. Molecular masses were determined by running a Broad Range Protein Marker (Bio-Rad, Hercules, CA) at the sides of selected gels. p*I* values were calculated according to the instructions of the manufacturer of the Immobiline DryStrips. Observed molecular mass and isoelectric point were determined with PDQUEST (Bio-Rad). Scatter plot analysis for pair-wise overall comparison was also performed with PDQUEST (Bio-Rad).

2.5. In-gel proteolytic digestion and mass spectrometry analysis for protein identification

The position of selected spots was recorded as a text file by use of DeCyder software. An automated spot collector, SpotPicker (Amersham Biosciences), excised the spots according to the content of the text file and transferred the gel plugs to 96-well plates. In-gel proteolytic digestion was carried out as described previously, with some modifications [16]. Briefly, the gel plugs were washed twice for 5 min with Milli Q water (Millipore, Bedford, MA) and then incubated with 100% acetonitrile for 10 min. After completely drying the gels with a SpeedVac (Thermo Savant, Holbrook, NY), the protein in the gel was digested overnight with 100 ng of TPCK-treated trypsin (Promega, Southampton, UK) in 50 mM ammonium bicarbonate at 37 °C for 3 h with gentle agitation. Following digestion, peptides were extracted with 50 μl of 50% acetonitrile/0.1% TFA, twice, and concentrated with the SpeedVac. A 1 μl sample of extracted peptides was then mixed with an equal volume of matrix solution composed of saturated dihydroxybenzoic acid (DHB) in 50% acetonitrile/0.1% TFA. The mixture was spotted onto a target plate and subjected to mass spectrometry analysis.

Protein identification by matrix-assisted laser desorption/ionization time-of-flight mass spectrometry (MALDI-TOF) was performed with a Q-Star Pulser-i equipped with the oMALDI ion source (Applied Biosystems, Framingham, CA). We optimized various parameters including pulse rate, power level, collision energy/gas, depending on the samples and the ion peaks. All mass spectra were externally calibrated with a mixture of the three peptides included in the Sequenzyme Peptide Mass Standards kit (Applied Biosystems): des-arg1-bradykinin (Mr 904.4681), angiotensin I (Mr 1296.6853) and glu1-fibrinopeptide B (Mr 1570.6774). Mass spectra were processed with the Analyst QS program (Applied Biosystems). A minimum of a 5-peptide match, a maximum of 1 miscleavage, and cysteine modifications by acrylamide were used for peptide mass fingerprinting (PMF). A search of the SWISS-PROT database was performed with a mass tolerance of 100 ppm by using the Analyst QS program (Applied Biosystems). When PMF did not result in an unambiguous identification, selected peptides were subjected to MS/MS analysis. When the results by both MS and MS/MS analysis were consistent, the identification was considered as positive. The theoretical Mr and p*I* were obtained from the SWISS-PROT database. Results of identification by PMF and MS/MS data were scored by the Analyst QS and Mascot programs, and the top-scoring gene products were considered to be the corresponding proteins.

2.6. Functional classification of identified proteins

The identified proteins were functionally categorized according to Panther Category. In brief, the SWISS-PROT entry name of the identified proteins was entered into the Celera Discovery System (http://www.celera.com). We searched how the identified proteins were categorized in the database and the results were summarized in Table 2.

2.7. Dephosphorylation of proteins by phosphatase treatment

Proteins were dephosphorylated by treatment with calf intestinal alkaline phosphatase (CIAP; New England Biolabs, Beverly, MA). Briefly, a 750 μg protein sample was diluted with a reaction buffer consisting of 1 M NaCl, 0.1 M $MgCl_2$, 10 mM DTT and 0.5 M Tris (pH 7.9) and divided into two equal volumes. Then, 10 μl of CIAP (10 U/μl) diluted in CIAP buffer, consisting of 50 mM KCl, 1 mM $MgCl_2$, 0.1 mM $ZnCl_2$ and 10 mM Tris (pH 8.2), was added to one sample, and 10 μl of the CIAP buffer lacking CIAP was added to the other sample. After incubation at 37 °C for 15 min, the reaction was terminated by addition of urea lysis buffer. The samples were labeled with Cy3 and Cy5 fluorescence dyes, respectively, mixed together and separated by 2D-PAGE in the same gel as described above. Pair-wise overall comparison of spot intensity was performed by scatter plot analysis using PDQUEST (Bio-Rad).

2.8. Pair-wise comparison of 2D images from DLD-1 cells and colon cancer cells

Protein samples from DLD-1 cells and from microdissected colon cancer tissue were labeled with Cy3 and Cy5 fluorescent dyes, respectively, and subjected to 2D-PAGE as described above. Pair-wise overall comparison was performed by scatter plot analysis as described above.

3. Results

3.1. Identification of fluorescence-labeled protein spots by MALDI-TOF

Among the protein spots present in both the quantitative and analytical gels, approximately 500 spots were chosen without regard to their intensity and subjected to in-gel proteolytic digestion followed by mass spectrometry analysis. Protein identification was first achieved by PMF and, for some proteins, the results were further confirmed by MS/MS analysis. We finally identified the proteins corresponding to 314 protein spots listed in Table 1. Fig. 1 shows a representative 2D pattern of fluorescence-labeled proteins of DLD-1 cells with the spot numbers of the identified proteins. A representative mass spectrometric pattern of trypsin digests from spot 216 is shown in Fig. 2A. Processing of ion peaks and a database search resulted in the identification of spot 216 as Rho GDP-dissociation inhibitor 1 (Fig. 2B). Mass spectrometry analysis was performed on the other protein spots, and the spots with sufficient peptide coverage to obtain positive protein identification are listed in Table 1.

3.2. Classification of identified proteins

We grouped the identified protein spots according to Panther Category by accessing the Celera Discovery System (Table 2). The majority of the proteins belonged to the oxidoreductase (10.5%), cytoskeletal protein (9.4%), nucleic acid binding protein (8.9%), chaperone (7.0%) and isomerase (6.7%) families (Table 2). In this study, members of certain protein families, including transcription factors, transporters, membrane traffic proteins and viral proteins,

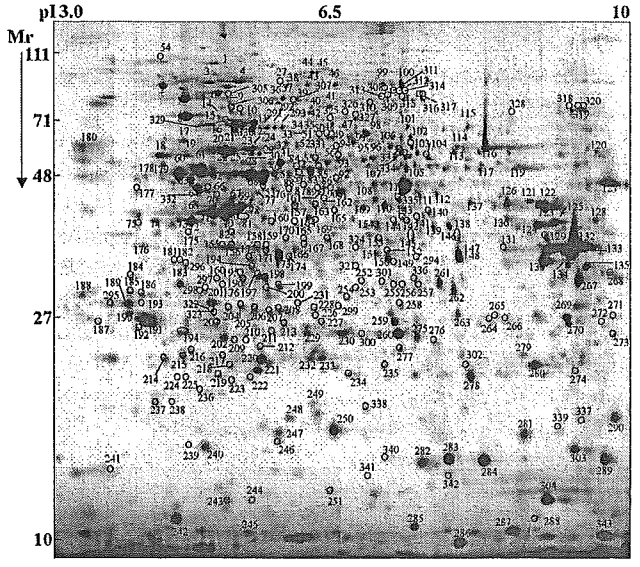

Fig. 1. A representative 2D image of Cy5-labeled proteins extracted from DLD-1 cells. The total number of spots observed is approximately 1500. The numbers assigned to the protein spots are those shown in Table 1. Proteins not identified by mass spectrometry analysis are not numbered in this figure.

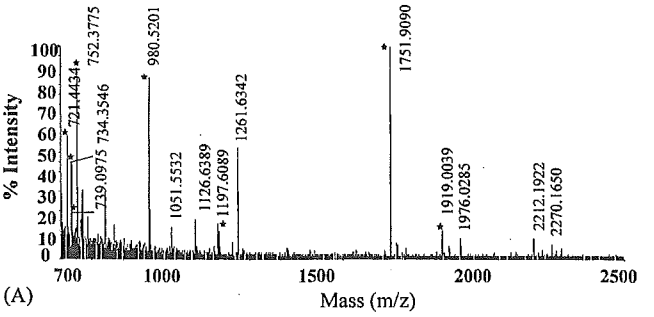

(A)

Rho GDP-dissociation inhibitor 1

(B)

MAEQEPTAEQ LAQIAAENEE DEHSVNYKPP AQKSIQEIQE
LDKDDESLRK YKEALLGRVA VSADPNVPNV VVTGLTLVCS
SAPGPLELDL TGDLESFKKQ SFVLKEGVEY RIKISFRVNR
EIVSGMKYIQ HTYRKGVKID KTDYMVGSYG PRAEEYEFLT
PVEEAPKGML ARGSYSIKSR FTDDDKTDHL SWEWNLTIKK
DWKD

Fig. 2. (A) Mass spectrogram of spot no. 216 in Fig. 1. A total of eight peptides (indicated by asterisks) are assigned to those of Rho GDP-dissociation inhibitor 1. (B) The peptide sequences corresponding to the peptide peaks in the mass spectrogram are underlined. The amino acid sequence coverage is 49.5%.

were not observed. However, these proteins may exist in the range of 2D-PAGE and the reason why they were not observed is probably because their expression level was lower than the detection limit of Cy5 fluorescent dye. Based on the genome database, Medjahed et al. constructed the virtual 2D image; they calculated p*I* and molecular weight of gene products and plotted the products in two-dimensional space [18]. According to their data, p*I* and molecular weight of most of proteins distributed within the range of 2D-PAGE. More extensive study such as sample fractionation prior to electrophoresis may visualize these lower abundant proteins. Our data showed that some regulatory proteins such as kinases and receptors, which are generally expressed in small amounts, were already identified in 2D gel. Therefore, 2D-PAGE has a potential to uncover most of proteome and increasing the sensitivity for spot detection should be the critical issue of developing 2D-DIGE. Since 2D imaging of fluorescence-labeled proteins allows monitoring of proteins from a broad spectrum of functions, it represents a powerful tool for initial study of the proteome and will be useful for biological studies in which quantitative expression profiles are required.

3.3. Redundancy of identified proteins and prediction of total number of proteins

We looked into Table 1 and found that, among the 314 protein spots identified, 52 gene products appeared more than once (Table 3). Post-translational modifications, including phosphorylation, splicing variation, and glycation, can result in more than one protein spot from the same gene. To estimate the contribution of phosphorylation to spot redundancy in our 2D gels, the protein sample was dephosphorylated by phosphatase treatment and subjected to 2D separation. 2D images of proteins with or without phosphatase treatment

Table 1

Spot no.[a]	Access. no.[b]	Swiss-prot name[c]	Protien description[d]	Theoretical[e] (Mr/pI)	Experimental[f] (Mr/pI)	Sequence[g] coverage (%)
Nucleic acid binding						
20	Q07244	ROK_HUMAN	Heterogeneous nuclear ribonucleoprotein K (hnRNP K)	51.3/5.28	60.5/5.29	32.1
23	Q07244	ROK_HUMAN	Heterogeneous nuclear ribonucleoprotein K (hnRNP K)	51.3/5.28	61.1/5.58	33.5
71	P08865	RSP4_HUMAN	40S ribosomal protein SA (P40)	33.0/4.62	43.7/4.72	50.8
78	P55795	ROH2_HUMAN	Heterogeneous nuclear ribonucleoprotein H′ (HNRNP H′)	49.5/6.26	53.4/6.21	30.5
86	P26641	EF1G_HUMAN	Elongation factor 1-gamma (EF-1-gamma)	50.5/6.64	50.2/6.32	43.2
87	P38919	IF4N	Eukaryotic initiation factor 4A-like NUK-34	47.1/6.4	50.5/6.47	11.9
90	P49591	SYS_HUMAN	Seryl-tRNA synthetase (serine-tRNA ligase)	59.3/6.39	59.2/6.46	28.6
94	P13639	EF2_HUMAN	Elongation factor 2 (EF-2)	96.2/6.8	96.6/6.92	38.6
95	P13639	EF2_HUMAN	Elongation factor 2 (EF-2)	96.2/6.8	96.1/7.12	43.5
97	P14866	ROL_HUMAN	Heterogeneous nuclear ribonucleoprotein L (hnRNP L)	60.8/7.1	63.2/7.22	9.4
103	P49411	EFTU_HUMAN	Elongation factor Tu, mitochondrial precursor (P43)	49.9/7.6	48.2/6.80	11.5
114	P04720	EF11_HUMAN	Elongation factor 1-alpha 1 (EF-1-alpha-1)	50.5/9.71	58.5/9.02	11.5
126	P22626	ROA2_HUMAN	Heterogeneous nuclear ribonucleoproteins A2/B1	37.5/9.77	34.8/8.65	18.1
127	P22626	ROA2_HUMAN	Heterogeneous nuclear ribonucleoproteins A2/B1	37.5/9.77	34.6/8.87	24.4
135	Q15365	PCB1_HUMAN	Poly (rC)-binding protein 1 (Alpha-CP1)	38.0/7.17	42.1/7.03	46.9
141	P05388	RLA0_HUMAN	60S Acidic ribosomal protein P0 (L10E)	34.4/5.83	35.9/6.59	28.7
145	P05198	IF2A_HUMAN	Eukaryotic translation initiation factor 2 subunit 1 (EIF-2A)	36.4/4.84	39.3/5.27	35.2
148	Q13347	IF32_HUMAN	Eukaryotic translation initiation factor 3 subunit 2	36.9/5.44	38.1/5.64	35.4
149	Q13347	IF32_HUMAN	Eukaryotic translation initiation factor 3 subunit 2	36.9/5.44	38.5/5.75	35.4
168	P54727	R23B_HUMAN	UV excision repair protein RAD23 homolog B (HHR23B)	43.2/4.6	53.2/4.77	18.1
170	P29692	EF1D_HUMAN	Elongation factor 1-delta (EF-1-delta)	31.3/4.97	36.4/4.89	25.6
171	P29692	EF1D_HUMAN	Elongation factor 1-delta (EF-1-delta)	31.3/4.97	36.4/4.97	17.1
173	P12004	PCNA_HUMAN	Proliferating cell nuclear antigen (PCNA) (Cyclin)	29.1/4.4	34.8/4.45	28.0
194	Q13347	IF32_HUMAN	Eukaryotic translation initiation factor 3 subunit 2	36.9/5.44	29.4/5.76	46.8
229	Q15056	IF4H_HUMAN	Eukaryotic translation initiation factor 4H (eIF-4H)	27.4/6.67	32.4/6.52	31.0
239	Q07955	SFR1_HUMAN	Splicing factor, arginine/serine-rich 1	27.9/6.48	29.9/7.92	45.6
266	P24534	EF1B_HUMAN	Elongation factor 1-beta (EF-1-beta)	24.8/4.33	32.1/4.14	63.8
270	Q15056	IF4H_HUMAN	Eukaryotic translation initiation factor 4H (eIF-4H)	27.4/6.67	31.5/6.45	8.6
281	O00571	DDX3_HUMAN	DEAD-box protein 3 (Helicase-like protein 2)	73.5/7.17	80.3/6.77	34.3
286	O00571	DDX3_HUMAN	DEAD-box protein 3 (Helicase-like protein 2)	73.5/7.17	84.6/7.14	34.3
298	P12956	KU70_HUMAN	ATP-dependent DNA helicase II, 70 kDa subunit (Ku70)	70.0/6.61	73.3/6.61	37.3
299	P11940	PAB1_HUMAN	Polyadenylate-binding protein 1	70.9/10.31	79.6/8.29	18.4
313	Q99880	H2BC_HUMAN	Histone H2B.c (H2B/c)	13.8/11.13	13.8/7.67	75.2
Oxidoreductase						
21	P07237	PDI_HUMAN	Protein disulfide isomerase precursor (PDI)	57.5/4.59	60.5/5.29	32.1
33	P48163	MAOX_HUMAN	NADP-dependent malic enzyme (NADP-ME)	64.7/6.04	63.1/5.94	10.1
46	P31040	DHSA_HUMAN	Succinate dehydrogenase (ubiquinone) flavoprotein subunit	73.7/7.34	70.0/6.59	27.1
74	P31930	UCR1_HUMAN	Ubiquinol-cytochrome C reductase complex core protein I	53.3/6.33	49.8/5.67	16
80	P30837	DHA5_HUMAN	Aldehyde dehydrogenase X, mitochondrial precursor (ALDH class 2)	57.7/6.83	54.7/6.28	30.4
91	O43175	SERA_HUMAN	D-3-Phosphoglycerate dehydrogenase (PGDH)	57.4/6.68	56.8/6.69	7.5
98	O60701	UGDH_HUMAN	UDP-glucose 6-dehydrogenase (UDP-glc dehydrogenase)	55.7/7.08	58.9/7.23	20.4
100	P00367	DHE3_HUMAN	Glutamate dehydrogenase 1, mitochondrial precursor (GDH)	61.7/7.82	54.1/7.17	12.2
101	P11413	G6PD_HUMAN	Glucose-6-phosphate 1-dehydrogenase (G6PD)	59.7/6.87	59.1/6.99	31.3
104	O75874	IDHC_HUMAN	Isocit rate dehydrogenase (NADP) cytoplasmic	47.0/6.79	46.8/6.88	19.1
105	O75874	IDHC_HUMAN	Isocit rate dehydrogenase (NADP) cytoplasmic	47.0/6.79	46.7/6.91	22.0
122	P00338	LDHA_HUMAN	L-lactate dehydrogenase A chain (LDH-A)	37.0/8.34	35.2/8.42	66.3
123	P04406	G3P2_HUMAN	Glyceraldehyde 3-phosphate dehydrogenase, liver	36.2/8.73	36.4/8.06	43.3
124	P04406	G3P2_HUMAN	Glyceraldehyde 3-phosphate dehydrogenase, liver	36.2/8.73	36.2/8.74	43.3
125	P04406	G3P2_HUMAN	Glyceraldehyde 3-phosphate dehydrogenase, liver	36.2/8.73	36.2/8.74	43.3
136	P36551	HEM6_HUMAN	Coproporphyrinogen III oxidase, mitochondrial precursor	40.9/7.11	38.3/7.24	46.9
140	P40925	MDHC_HUMAN	Malate dehydrogenase, cytoplasmic	36.7/7.37	35.6/7.04	21.0
141	P40925	MDHC_HUMAN	Malate dehydrogenase 1, NAD (soluble)	36.4/6.91	35.9/6.59	43.5
144	P14550	ALDX_HUMAN	Alcohol dehydrogenase [NADP+] (Aldehyde reductase)	36.9/6.78	38.8/6.86	33.5
159	O75874	IDHC_HUMAN	Isocitrate dehydrogenase (NADP) cytoplasmic	47.0/6.79	39.2/5.92	52.7
159	O75874	IDHC_HUMAN	Isocitrate dehydrogenase 3 (NAD+) alpha	47.0/6.79	39.2/5.92	20.0
162	P07195	LDHB_HUMAN	L-lactate dehydrogenase B chain (LDH-B)	36.9/5.96	36.7/5.84	31.7
162	P07195	LDHB_HUMAN	L-lactate dehydrogenase B chain (LDH-B	36.9/5.96	36.7/5.84	40.7
203	P32119	PDX2_HUMAN	Peroxiredoxin 2 (Thioredoxinperoxidase 1)	22.1/5.8	26.4/5.61	44.9
210	P30041	AOP2_HUMAN	Antioxidant protein 2 (1-cis peroxiredoxin)	25.1/6.31	29.3/6.47	69.2
212	P30048	PDX3_HUMAN	Peroxiredoxin 3; antioxidant protein 1	27.7/7.67	27.4/6.16	5.0
230	P13804	ETFA_HUMAN	Electron transfer flavoprotein alpha-subunit	35.4/8.44	33.4/7.04	23.4

Table 1 (*Continued*)

Spot no.[a]	Access. no.[b]	Swiss-prot name[c]	Protien description[d]	Theoretical[e] (Mr/p*I*)	Experimental[f] (Mr/p*I*)	Sequence[g] coverage (%)
231	P13804	ETFA_HUMAN	Electron transfer flavoprotein alpha-subunit	35.4/8.44	33.5/7.27	23.4
232	P13804	ETFA_HUMAN	Electron transfer flavoprotein alpha-subunit	35.4/8.44	33.4/7.47	23.4
235	P31930	UCR1_HUMAN	Ubiquinol-cytochrome C reductase complex core protein I	53.3/6.33	29.0/7.05	24.1
249	Q99714	HCD2_HUMAN	3-Hydroxyacyl-CoA dehydrogenase type II (Type II HADH)	27.2/7.79	28.3/7.36	26.1
253	Q06830	PDX1_HUMAN	Peroxiredoxin 1 (Thioredoxin peroxidase 2)	22.3/8.18	26.3/8.33	41.2
254	P30044	PDX5_HUMAN	Peroxiredoxin 5, mitochondrial	22.1/8.85	16.3/7.40	5.6
267	O43396	TXNL_HUMAN	Thioredoxin-like protein (32 kDa thioredoxin-related protein)	32.7/4.67	35.8/5.01	38.8
271	P31930	UCR1_HUMAN	Ubiquinol-cytochrome C reductase complex core protein I	53.3/6.33	29.3/6.47	24.1
273	Q06830	PDX1_HUMAN	Peroxiredoxin 1 (Thioredoxin peroxidase 2)	22.3/8.18	26.2/7.70	39.2
283	P28331	NUAM_HUMAN	NADH-ubiquinone oxidoreductase 75 kDa	80.6/5.98	88.1/7.13	23.9
304	O60701	UGDH_HUMAN	UDP-glucose 6-dehydrogenase (UDPGDH)	55.7/7.08	57.9/7.11	35.8
307	P13804	ETFA_HUMAN	Electron transfer flavoprotein alpha-subunit	35.4/8.44	33.5/7.27	35.4
Cytoskeletal protein						
5	O43707	AAC4_HUMAN	Alpha-actinin 4 (F-actin cross linking protein)	105.3/5.21	99.1/5.4	7.1
16	P20700	LAM1_HUMAN	Lamin B1	66.7/4.94	70.4/5.27	54.1
34	P04264	K2C1_HUMAN	Keratin, type II cytoskeletal 1 (CK 1)	66.2/8.33	68.1/6.01	13.8
37	P06396	GELS_HUMAN	Gelsolin precursor, plasma	86.1/5.90	88.6/5.9	13.6
39	P15311	EZRI_HUMAN	Ezrin (p81) (cytovillin) (villin2)	69.5/6.2	81.1/6.2	29.0
40	P15311	EZRI_HUMAN	Ezrin (p81) (cytovillin) (villin2)	69.5/6.2	81.8/6.38	33.4
42	P35221	CTN1_HUMAN	Alpha-1 catenin	100.8/6.2	98.8/6.16	14.3
43	P18206	VINC_HUMAN	Vinculin (metavinculin)	117.3/8	110.1/6.21	8.4
44	P18206	VINC_HUMAN	Vinculin (metavinculin)	117.3/8	110.1/6.26	8.4
52	P35900	K1CT_HUMAN	Keratin, type I cytoskeletal 20	48.5/5.52	50.6/5.64	3.1
57	P05787	K2C8_HUMAN	Keratin, typeII cytoskeletal 8 (CK 8)	53.7/5.37	55.9/5.70	91.6
58	P05217	TBB2_HUMAN	Tubulin beta-2 chain	50.3/4.63	53.1/4.97	52.4
59	P05209	TBA1_HUMAN	Tubulin alpha-1 chain, brain-specific	50.8/4.89	55.4/5.16	45.7
65	P05787	K2C8_HUMAN	Keratin, typeII cytoskeletal 8 (CK 8)	53.7/5.37	53.7/5.57	42.8
66	P05783	K1CR_HUMAN	Keratin, type I cytoskeletal 18 (CK 18)	48.5/5.22	47.4/5.50	77.4
67	P02570	ACTB_HUMAN	Actin, cytoplasmic 1 (beta-actin)	42.1/5.24	45.3/5.24	48.0
68	P02570	ACTB_HUMAN	Actin, cytoplasmic 1 (beta-actin)	42.1/5.42	46.0/5.14	50.3
69	P08727	K1CS_HUMAN	Keratin, type I cytoskeletal 19 (CK 19)	44.1/4.89	43.6/5.07	27.5
70	P08727	K1CS_HUMAN	Keratin, type I cytoskeletal 19 (CK 19)	44.1/4.89	44.1/4.06	90.3
71	P08727	K1CS_HUMAN	Keratin, type I cytoskeletal 19 (CK 19)	44.1/4.89	43.7/4.72	90.3
73	P32391	ARP3_HUMAN	Actin-like protein 3 (Actin-related protein 3)	47.8/5.74	48.4/5.87	30.1
76	P02570	ACTB_HUMAN	Actin, cytoplasmic 1 (beta-actin)	42.1/5.24	43.7/5.34	25.6
77	P05783	K1CR_HUMAN	Keratin, type I cytoskeletal 18 (CK 18)	48.5/5.22	45.2/5.35	20.2
109	O75083	WDR1_HUMAN	WD-repeated protein 1	66.9/6.64	68.8/7.74	5.9
154	Q15019	SEP2_HUMAN	Septin 2	41.7/6.58	45.3/6.43	32.1
161	P52907	CAZ1_HUMAN	F-actin capping protein alpha-1 subunit	33.1/5.5	35.9/5.57	52.4
174	P12324	TPMN_HUMAN	Tropomyosin, cytoskeletal type	29.3/4.56	33.2/4.42	39.5
175	P12324	TPMN_HUMAN	Tropomyosin, cytoskeletal type	29.3/4.59	32.9/4.58	52.4
181	P10469	TPMS_HUMAN	Tropomyosin alpha chain, smooth muscle	26.6/4,59	31.1/4.58	32.2
188	P47756	CAPB_HUMAN	F-actin capping protein beta subunit	31.0/5.82	33.0/5.72	59.9
275	P007737	PRO1_HUMAN	Profilin I	15.1/8.35	11.6/8.46	64.0
277	Q14247	SRC8_HUMAN	Src substrate cortactin	61.8/5.14	81.3/5.43	54.0
280	P02545	LAMA_HUMAN	Lamin A/C (70 kDa lamin)	74.4/7.0	85.3/6.97	32.8
284	P02545	LAMA_HUMAN	Lamin A/C (70 kDa lamin)	74.4/7.0	81.7/6.92	54.7
301	Q03252	LAM2_HUMAN	Lamin B2	66.9/6.03	70.8/5.46	69.1
Chaperone						
1	Q9Y4L1	OXRP_HUMAN	150 kDa oxygen-regulated protein precursor	111.6/5.0	119.6/5.26	9.1
2	P14625	ENPL_HUMAN	Endoplasmin precursor (GRP94)	92.8/4.58	98.6/4.79	6.0
7	P07900	HS9A_HUMAN	Heat shock protein HSP 90-alpha (HSP 86)	85.1/4.77	87.2/5.02	10.0
8	P11021	GR78_HUMAN	78 kD glucose regulated protein precursor (GRP 78)	72.2/4.86	76.2/5.04	48.1
11	P38646	GR75_HUMAN	Mitochondrial stress-70 protein precursor (GRP 75)	74.1/6.21	72.8/5.61	29.9
12	P08107	HS71_HUMAN	Heat shock 70 kDa protein 1 (HSP70.1)	70.3/5.4	69.1/5.58	31.4
15	P11142	HS7C_HUMAN	Heat shock cognate 71 kDa protein	71.1/5.25	73.0/5.19	71.1
22	P10809	CH60_HUMAN	60 kDa heat shock protein, mitochondrial precursor (Hsp60)	61.2/5.46	58.5/5.37	46.4
24	P48643	TCPE_HUMAN	T-complex protein 1, epsilon subunit (TCP-1-epsilon)	60.1/5.42	58.7/5.66	31.6
25	P54578	UBPE_HUMAN	Ubiquitin carboxyl-terminal hydrolase 14	55.9/5.20	59.3/5.42	4.9
26	P50990	TCPQ_HUMAN	T-complex protein 1, theta subunit	59.6/5.20	58.5/5.58	22.3
27	P14625	ENPL_HUMAN	Endoplasmin precursor (GRP94)	92.8/4.58	99.1/5.89	4.5
29	P50990	TCPQ_HUMAN	T-complex protein 1, theta subunit (TCP-1-theta)	60.2/5.39	58.7/5.66	22.3

Table 1 (*Continued*)

Spot no.[a]	Access. no.[b]	Swiss-prot name[c]	Protien description[d]	Theoretical[e] (Mr/p*I*)	Experimental[f] (Mr/p*I*)	Sequence[g] coverage (%)
32	P11142	HS7C_HUMAN	Heat shock cognate 71 kDa protein	71.1/5.25	66.2/5.79	71.1
36	P07900	HS9A_HUMAN	Heat shock protein HSP 90-alpha (HSP 86)	85.1/4.77	87.9/5.81	10.0
38	P14625	ENPL_HUMAN	Endoplasmin precursor (GRP94)	92.8/4.58	98.6/5.94	31.0
47	P49368	TCPG_HUMAN	T-complex protein 1, gamma subunit (TCP-1-gamma)	60.9/6.6	64.9/6.36	41.2
51	P17987	TCPA_HUMAN	T-complex protein 1, alpha subunit (TCP-1-alpha)	60.9/6.0	61.8/6.05	23.4
54	P78371	TCPB_HUMAN	T-complex protein 1, beta subunit (TCP-1-beta)	57.8/6.42	55.7/5.87	40.4
56	P78371	TCPB_HUMAN	T-complex protein 1, beta subunit (TCP-1-beta)	57.8/6.42	53.3/5.83	26.4
93	P31948	IEFS_HUMAN	Stress-induced-phosphoprotein I (STI1)	63.3/6.77	84.3/6.73	54.1
107	5453607	TCPH_HUMAN	Chaperonin containing TCP1, subunit 7 (eta)	59.4/7.55	57.7/7.60	10.0
209	P04792	HS27_HUMAN	Heat shock protein 27 kDa protein (HSP 27)	22.4/8.14	29.4/6.14	54.3
279	P08238	HS9B_HUMAN	Heat shock protein HSP 90-beta (HSP 84) (HSP 90)	83.5/4.79	94.4/6.81	49.8
282	P07900	HS9A_HUMAN	Heat shock protein HSP 90-alpha (HSP 86)	84.9/4.77	88.4/7.04	10.0
314	Q04984	CH10_HUMAN	10 kDa heat shock protein, mitochondrial (Hsp10)	10.8/9.73	9.2/8.98	56.4
Miscellaneous function						
16	P20700	LAM1_HUMAN	Lamin B1	66.7/4.94	70.4/5.27	54.1
57	P05787	K2C8_HUMAN	Keratin, typeII cytoskeletal 8 (CK 8)	53.7/5.37	55.9/5.70	71.6
65	P05787	K2C8_HUMAN	Keratin, typeII cytoskeletal 8 (CK 8)	53.67/5.37	53.7/5.57	42.8
66	P05783	K1CR_HUMAN	Keratin, type I cytoskeletal 18 (CK 18)	48.5/5.22	47.4/5.50	77.4
69	P08727	K1CS_HUMAN	Keratin, type I cytoskeletal 19 (CK 19)	44.1/4.89	43.6/5.07	27.5
70	P08727	K1CS_HUMAN	Keratin, type I cytoskeletal 19 (CK 19)	44.1/4.89	44.1/4.06	90.3
71	P08727	K1CS_HUMAN	Keratin, type I cytoskeletal 19 (CK 19)	44.1/4.89	43.7/4.72	90.3
77	P05783	K1CR_HUMAN	Keratin, type I cytoskeletal 18 (CK 18)	48.5/5.22	45.2/5.35	20.2
164	Q9Y3F4	UNRI_HUMAN	UNR-interacting protein (WD-40 repeat protein PT-WD)	38.8/4.85	41.2/5.05	32.9
177	P42655	143E_HUMAN	14-3-3 protein epsilon	29.3/4.46	32.1/4.41	55.7
188	P47756	CAPB_HUMAN	F-actin capping protein beta subunit	31.0/5.82	33.0/5.72	59.9
193	P42168	IGUP_HUMAN	Interferon gamma up-regulated I-5111 protein	28.9/5.9	31.3/5.84	68.7
195	P52566	GDIS_HUMAN	Rho GDP-dissociation inhibitor 2 (Rho GDI 2)	23.0/4.94	28.0/5.63	19.9
224	P16949	STN1_HUMAN	Stathmin	17.3/5.76	19.8/5.81	11.0
237	P25388	GBLP_HUMAN	Guanine nucleotide-binding protein beta subunit-like protein 12.3	35.5/7.64	32.7/7.60	20.8
268	Q15691	MAE1_HUMAN	Microtubule-associated protein RP/EB family member 1	30.2/4.86	33.3/5.17	26.9
280	P02545	LAMA_HUMAN	Lamin A/C (70 kDa lamin)	74.4/7.0	85.3/6.97	32.8
284	P02545	LAMA_HUMAN	Lamin A/C (70 kDa lamin)	74.4/7.0	81.7/6.92	54.7
Isomerase						
18	P07237	PDI_HUMAN	Protein disulfide isomerase precursor (PDI)	57.5/4.59	59.2/4.77	32.7
18	P07237	PDI_HUMAN	Protein disulfide isomerase precursor (PDI)	57.5/4.59	59.2/4.77	32.7
21	P07237	PDI_HUMAN	Protein disulfide isomerase precursor (PDI)	57.5/4.59	60.5/5.29	32.7
28	P30101	PDA3_HUMAN	Protein disulfide isomerase A3 precursor	57.2/6.29	56.6/5.5	35.6
28	Q02790	FKB4_HUMAN	P59 protein (HSP binding immunophilin)	52.1/5.24	56.6/5.5	17.9
28	P30101	PDA3_HUMAN	Protein disulfide isomerase A3 precursor	57.2/6.29	56.6/5.5	35.6
30	P30101	PDA3_HUMAN	Protein disulfide isomerase A3 precursor	57.2/6.29	57.1/5.77	54.1
30	P30101	PDA3_HUMAN	Protein disulfide isomerase A3 precursor	57.2/6.29	57.1/5.77	54.1
31	P30101	PDA3_HUMAN	Protein disulfide isomerase A3 precursor	57.2/6.29	50.8/5.87	35.6
31	P30101	PDA3_HUMAN	Protein disulfide isomerase A3 precursor	57.2/6.29	50.8/5.87	35.6
50	O95394	AGM1_HUMAN	Phosphoacetylglucosamine mutase (PAGM)	60.3/6.22	64.7/6.11	20.3
133	Q08752	CYP4_HUMAN	40 kDa peptidyl-prolyl cis-trans isomerase	41.2/7.19	42.2/7.18	21.1
234	P18669	PMG1_HUMAN	Phosphoglycerate mutase, muscle form (PGAM-B)	28.9/7.2	31.2/7.10	30.3
234	P15259	PMGM_HUMAN	Phosphoglycerate mutase, muscle form (PGAM-M)	28.9/9.5	30.1/7.01	22.1
235	P00938	TPIS_HUMAN	Triosephosphate isomerase (TIM)	27.0/6.89	29.0/7.05	67.1
246	Q00688	FKB3_HUMAN	Rapamycin-selective 25 kDa immunophilin (FKBP25)	25.2/10.07	30.2/9.11	17.9
255	P05092	CYPH_HUMAN	Peptidyl-prolyl cis-trans isomerase A (PPIase)	11.2/7.68	16.6/7.53	45.9
256	P05092	CYPH_HUMAN	Peptidyl-prolyl cis-trans isomerase A (PPIase)	18.2/7.83	16.3/7.85	40.0
259	P20071	FKB1_HUMAN	FK506-binding protein 1A; FK506-binding protein 1A	11.9/8.08	10.2/8.35	5.6
261	P23284	CYPB_HUMAN	Peptidyl-prolyl cis-trans isomerase B precursor (PPIase	22.8/10.11	22.8/9.10	43.8
295	Q14376	GALE_HUMAN	UDP-glucose 4-epimerase (Galactowaldenase)	38.7/6.7	37.1/6.65	15.2
305	P30101	PDA3_HUMAN	Protein disulfide isomerase A3 precursor	57.2/6.29	56.6/7.15	23.2
305	P30101	PDA3_HUMAN	Protein disulfide isomerase A3 precursor	57.2/6.29	56.6/7.15	23.2
308	P30405	CYPM_HUMAN	Peptidyl-prolyl cis-trans isomerase	22.7/9.72	22.4/8.82	7.7
311	P05092	CYPH_HUMAN	Peptidyl-prolyl cis-trans isomerase A (PPIase)	11.2/7.68	16.6/7.53	14.6
Select calcium binding						
37	P06396	GELS_HUMAN	Gelsolin precursor, plasma (ADF)	86.1/5.90	88.6/5.9	13.6
72	Q15293	RCN1_HUMAN	Reticulocalbin 1 precursor	38.9/4.71	43.5/4.54	19.9

Table 1 (*Continued*)

Spot no.[a]	Access. no.[b]	Swiss-prot name[c]	Protien description[d]	Theoretical[e] (Mr/p*I*)	Experimental[f] (Mr/p*I*)	Sequence[g] coverage (%)
83	P20073	ANX7_HUMAN	Annexin A7	50.3/6.25	53.7/6.05	7.6
99	P50995	ANXB_HUMAN	Annexin A11 (Annexin XI)	54.7/7.66	56.5/7.36	32.9
129	P07355	ANX2_HUMAN	Annexin II (Lipocortin II)	38.8/7.82	38.5/8.46	45.4
137	P07355	ANX2_HUMAN	Annexin II (Lipocortin II)	38.8/7.82	38.6/7.61	41.3
138	P07355	ANX2_HUMAN	Annexin II (Lipocortin II)	38.8/7.82	36.4/7.00	58.7
139	P07355	ANX2_HUMAN	Annexin II (Lipocortin II)	38.8/7.82	35.7/7.61	58.7
142	P04083	ANX1_HUMAN	Annexin I (Lipocortin I)	38.9/7.02	36.7/6.81	78.3
143	P04083	ANX1_HUMAN	Annexin I (Lipocortin I)	38.9/7.02	36.7/7.02	78.3
150	P20073	ANX7_HUMAN	Annexin A7 (Annexin VII)	50.6/6.55	50.3/6.25	8.9
169	P27797	CRTC_HUMAN	Calreticulin precursor	48.3/4.12	69.0/3.98	20.9
172	P08758	ANX5_HUMAN	Annexin V (Lipocortin V)	36.0/4.76	33.9/4.95	52.8
182	P04632	CANS_HUMAN	Calcium-dependent protease, small subunit	28.5/4.91	29.5/4.95	28.4
184	P12429	ANX3_HUMAN	Annexin III (Lipocortin III)	36.5/5.76	34.1/5.52	56.0
186	P12429	ANX3_HUMAN	Annexin III (Lipocortin III)	36.5/5.76	34.2/5.71	65.6
187	P09525	ANX4_HUMAN	Annexin A4 (Annexin IV)	36.1/5.95	33.5/5.85	68.3
216	P19105	MLRM_HUMAN	Myosin regulatory light chain 2	19.7/4.48	24.2/4.68	18.8
262	P02769	ALBU_BOVIN	Serum albumin	69.3/5.82	69.4/5.72	45.0
263	P02769	ALBU_BOVIN	Serum albumin	69.3/5.82	69.4/5.84	55.6
264	P02769	ALBU_BOVIN	Serum albumin	69.3/5.82	69.4/5.93	36.3
265	P07355	ANX2_HUMAN	Annexin II (Lipocortin II)	38.8/7.82	36.1/7.25	41.3
Select regulatory molecule						
17	P30153	2AAA_HUMAN	Serine/threonine protein phosphatase 2A	66.0/4.81	63.0/5.00	25.1
19	P31150	GDIA_HUMAN	RAB GDP dissociation inhibitor alpha (RAB GDI alpha)	51.2/4.84	58.5/5.05	17.2
81	P50395	GDIB_HUMAN	RAB GDP dissociation inhibitor beta (RAB GDI beta)	51.1/6.15	51.3/6.32	14.6
81	P50395	GDIB_HUMAN	RAB GDP dissociation inhibitor beta (RAB GDI beta)	51.1/6.15	51.3/6.32	33.0
92	Q8WWP7	IMP1_HUMAN	Immunity-associated protein 1	34.4/9.11	55.8/6.80	4.3
103	P49411	EFTU_HUMAN	Elongation factor Tu, mitochondrial precursor (P43)	49.9/7.6	48.2/6.80	11.5
153	P30740	ILEU_HUMAN	Leukocyte elastase inhibitor (LEI)	42.9/6.21	44.6/6.16	43.3
170	P29692	EF1D_HUMAN	Elongation factor 1-delta (EF-1-delta)	31.3/4.97	36.4/4.89	25.6
171	P29692	EF1D_HUMAN	Elongation factor 1-delta (EF-1-delta)	31.3/4.97	36.4/4.97	17.1
179	P29312	143Z_HUMAN	14-3-3 Protein zeta/delta	27.9/4.54	30.1/4.65	100
179	P31946	143B_HUMAN	14-3-3 Protein beta/alpha	28.2/4.58	30.1/4.65	52.8
179	P27348	143T_HUMAN	14-3-3 Protein tau	28.0/4.51	30.1/4.65	31..0
179	Q04917	143F_HUMAN	14-3-3 Protein eta (Protein AS1)	28.4/4.58	30.1/4.65	43.1
182	P11016	GBB2_HUMAN	Guanine nucleotide-binding protein G(I)/G(S)/G(T) beta subunit 2	38.1/5.86	29.5/4.95	20.2
248	P17080	RAN_HUMAN	GTP-binding nuclear protein RAN	24.5/7.11	28.6/7.26	30.1
257	P04080	CYTB_HUMAN	Cystatin B (Liver thiol proteinase inhibitor)	11.2/7.68	10.0/7.23	45.9
309	P32889	ARF1_HUMAN	ADP-ribosylation factor 1	20.6/6.36	23.4/6.69	6.9
Transferase						
21	P07237	PDI_HUMAN	Protein disulfide isomerase precursor (PDI)	57.5/4.59	60.5/5.29	32.7
111	Q16851	UDP2_HUMAN	UTP-glucose-1-phosphote uridylyltransferase 2	57.1/7.69	54.4/7.73	18.1
115	P42765	THIM_HUMAN	3-Ketoacyl-CoA thiolase	42.5/8.24	47.0/8.29	21.2
116	P42765	THIM_HUMAN	3-Ketoacyl-CoA thiolase	42.5/8.24	45.9/8.37	21.2
130	Q9Y617	SERC_HUMAN	Phosphoserine aminotransferase (PSAT)	35.5/6.66	42.0/7.56	38.6
134	P17174	AATC_HUMAN	Aspartate aminotransferase, cytoplasmic	46.5/7.00	43.3/7.12	22.5
151	P04181	OAT_HUMAN	Ornithine aminotransferase	48.9/7.03	47.8/6.24	21
163	Q15274	NADC_HUMAN	Nicotinate-nucleotide pyrophosphorylase	31.3/6.16	35.7/5.97	18.5
290	P21266	GTM3_HUMAN	Glutathione S-transferase Mu 3	27.1/5.28	29.1/5.32	68.4
202	P09211	GTP_HUMAN	Glutathione S-transferase P	23.6/5.37	27.3/5.65	37.6
204	P07741	APT_HUMAN	Adenine phosphoribosyltransferase	19.6/5.88	25.7/5.54	24.6
211	P51580	TPMT_HUMAN	Thiopurine *S*-methyltransferase	28.6/6.18	32.1/6.08	22
227	P00491	PNPH_HUMAN	Purine nucleoside phosphorylase	32.4/6.94	33.5/6.68	69.6
292	P11908	KPR2_HUMAN	Phosphoribosyl pyrophosphate synthetase 2	34.7/6.15	34.7/6.63	36.4
Hydrolase						
4	P27815	CN4A_HUMAN	cAMP-specific 3′,5′-cyclic phosphodiesterase 4A	98.8/4.95	103.1/5.7	6.9
6	P55072	TERA_HUMAN	Transitional endoplasmic reticulum ATPase	90.0/4.99	94.0/5.31	38.7
10	P28331	NUAM_HUMAN	NADH-ubiquinone oxidoreductase 75 kDa subunit	80.6/5.98	80.3/5.51	21.7
35	P09960	LKHA_HUMAN	Leukotriene A-4 hydrolase	69.9/6.12	69.3/6.11	9.5
48	Q16555	DPY2_HUMAN	Dihydropyrimidinase related protein-2	62.8/6.34	64.0/6.41	24.8
49	Q16555	DPY2_HUMAN	Dihydropyrimidinase related protein-2	62.8/6.34	64.2/6.28	40.7
61	P06576	ATPB_HUMAN	ATP synthase beta chain	56.6/5.17	53.5/5.07	44.8

Table 1 (*Continued*)

Spot no.[a]	Access. no.[b]	Swiss-prot name[c]	Protien description[d]	Theoretical[e] (Mr/p*I*)	Experimental[f] (Mr/p*I*)	Sequence[g] coverage (%)
64	P06576	ATPB_HUMAN	ATP synthase beta chain	56.6/5.17	49.4/5.43	50.3
75	Q9Y2T3	GUAD_HUMAN	Guanine deaminase (Guanase)	51.5/5.52	50.1/5.58	37.9
100	P00367	DHE3_HUMAN	Glutamate dehydrogenase 1	61.7/7.82	54.1/7.17	12.2
152	P23526	SAHH_HUMAN	Adenosylhomocysteinase	48.3/6.44	47.3/6.41	12.7
183	Q15181	IPYR_HUMAN	Inorganic pyrophosphatase	33.1/5.68	34.8/5.50	64.7
185	Q15181	IPYR_HUMAN	Inorganic pyrophosphatase	33.1/5.68	34.7/5.64	53.6
272	P10768	ESTD_HUMAN	Esterase D	32.0/7.0	33.3/6.90	15.2
Protease						
4	P27815	CN4A_HUMAN	cAMP-specific 3′,5′-cyclic phosphodiesterase 4A	98.8/4.95	103.1/5.7	6.9
180	P28066	PSA5_HUMAN	Proteasome subunit alpha type 5	26.4/4.74	29.2/4.52	59.0
191	P07339	CATD_HUMAN	Cathepsin D precursor	45.1/6.5	31.6/5.38	23.1
213	P49720	PSB3_HUMAN	Proteasome (prosome, macropain) subunit, beta type, 3	22.9/6.14	27.3/6.28	43.0
214	P49721	PSB2_HUMAN	Proteasome (prosome, macropain) subunit, beta type, 2	22.8/6.52	26.0/6.53	43.0
215	P20618	PSB1_HUMAN	Proteasome subunit beta type 1	26.7/8.19	26.0/6.53	17.4
228	P25786	PSA1_HUMAN	Proteasome subunit alpha type 1	29.8/6.6	33.2/6.60	21.3
238	P25789	PSA4_HUMAN	Proteasome subunit alpha type 4	29.8/7.74	30.6/7.61	16.9
245	O15354	PSA7_HUMAN	Proteasome subunit alpha type 7	28.1/8.37	29.5/8.69	27.8
250	P25787	PSA2_HUMAN	Proteasome subunit alpha type 2	26.0/7.51	27.7/7.07	23.9
252	P20618	PSB1_HUMAN	proteasome subunit, beta type, 1	26.7/8.19	27.2/8.23	24.2
293	P25788	PSA3_HUMAN	Proteasome subunit alpha type 3	28.5/5.07	31.5/5.22	17.3
Kinase						
240	P06732	KCRM_HUMAN	Creatine kinase, M chain	43.1/6.77	30.4/7.98	40.0
274	P22392	NDKB_HUMAN	Nucleoside diphosphate kinase B	17.4/8.52	17.5/8.75	54.6
108	P14618	KPY1_HUMAN	Pyruvate kinase, M1 isozyme	58.4/7.62	59.0/7.65	23.7
110	P14618	KPY1_HUMAN	Pyruvate kinase, M1 isozyme	58.4/7.62	58.4/7.88	62.1
117	P00558	PGK1_HUMAN	Phosphoglycerate kinase 1	45.1/8.11	45.1/8.42	31.8
158	P51570	GAL1_HUMAN	Galactokinase (Galactose kinase)	42.7/6.45	43.0/6.30	43.1
162	O00764	PDXK_HUMAN	Pyridoxine kinase (Pyridoxal kinase)	35.3/6.07	36.7/5.84	26.0
225	P15531	NDKA_HUMAN	Nucleoside diphosphate kinase A	17.3/6.13	23.3/5.94	28.3
241	P54819	KAD2_HUMAN	Adenylate kinase isoenzyme 2	26.7/7.84	30.0/8.06	15.5
247	Q9UIJ7	KAD3_HUMAN	GTP: AMP phosphotransferase mitochondrial	25.6/10.14	28.8/9.11	20.7
292	P11908	KPR2_HUMAN	Phosphoribosyl pyrophosphate synthetase 2	34.7/6.15	34.7/6.63	31.5
Lyase						
33	P48163	MAOX_HUMAN	NADP-dependent malic enzyme (NADP-ME)	64.7/6.04	63.1/5.94	10.1
88	P06733	ENOA_HUMAN	Alpha enolase	47.5/7.38	52.2/6.45	47.5
102	P06733	ENOA_HUMAN	Alpha enolase	47.5/7.38	51.3/6.80	21.4
106	P07954	FUMH_HUMAN	Fumarate hydratase, mitochondrial precursor (Fumarase)	54.8/9.36	48.9/7.46	12.7
118	P04075	ALFA_HUMAN	Fructose-bisphosphate aldolase A	39.9/8.06	40.8/8.36	67
119	P04075	ALFA_HUMAN	Fructose-bisphosphate aldolase A	39.9/8.06	41.2/8.53	47.5
128	P06733	ENOA_HUMAN	Enolase 1; phosphopyruvate hydratase	47.5/7.38	43.0/8.07	67.8
129	O75390	CISY_HUMAN	Citrate synthase, mitochondrial precursor	51.7/8.45	46.4/7.74	37.6
198	Q04760	LGUL_HUMAN	Lactoylglutathione lyase	20.8/5.15	27.3/4.97	44.6
287	Q99798	ACON_HUMAN	Aconitate hydratase	86.2/7.57	85.3/7.36	24.6
288	Q99798	ACON_HUMAN	Aconitate hydratase	86.2/7.57	85.3/7.36	33.1
Synthase and synthetase						
41	P41250	SYG_HUMAN	Glycyl-tRNA synthetase	78.2/6.17	78.2/6.18	29.9
61	P06576	ATPB_HUMAN	ATP synthase beta chain	56.6/5.17	53.5/5.07	44.8
64	P06576	ATPB_HUMAN	ATP synthase beta chain	56.6/5.17	49.4/5.43	50.3
90	P49591	SYS_HUMAN	Seryl-tRNA synthetase	59.3/6.39	59.2/6.46	28.6
112	P22234	PUR6_HUMAN	Multifunctional protein ADE2	47.1/6.94	48.2/7.27	31.5
129	O75390	CISY_HUMAN	Citrate synthase	51.7/8.45	46.4/7.74	35.9
285	P47897	SYQ_HUMAN	Glutaminyl-tRNA synthetase	88.7/7.13	87.6/7.19	47.5
302	P23381	SYW_HUMAN	Tryptophanyl-tRNA synthetase	53.5/6.16	56.6/6.42	32.7
306	P22234	PUR6_HUMAN	Multifunctional protein ADE2	47.8/7.17	47.5/7.08	31.5
Cell adhesion molecule						
42	P35221	CTN1_HUMAN	Alpha-1 catenin	100.8/6.2	98.8/6.16	14.3
43	P18206	VINC_HUMAN	Vinculin	117.3/5.51	110.1/6.21	8.4
44	P18206	VINC_HUMAN	Vinculin	117.3/5.51	110.1/6.26	8.4
220	P09382	LEG1_HUMAN	Galectin-1	14.9/5.23	11.3/4.89	73.9
244	P17931	LEG3_HUMAN	Galectin-3	26.3/9.12	30.3/8.64	28.0

Table 1 (*Continued*)

Spot no.[a]	Access. no.[b]	Swiss-prot name[c]	Protien description[d]	Theoretical[e] (Mr/p*I*)	Experimental[f] (Mr/p*I*)	Sequence[g] coverage (%)
276	Q14126	DSG2_HUMAN	Desmoglein 2 precursor	123.1/5.03	90.0/5.41	19.7
Phosphatase						
155	P08129	PP1A_HUMAN	Serine/threonine protein phosphatase PP1-alpha 1	38.3/6.26	37.5/6.03	22.4
155	P36873	PP1G_HUMAN	Serine/threonine protein phosphatase PP1-gamma	37.7/6.49	37.5/6.03	19.8
155	P37140	PP1B_HUMAN	Serine/threonine protein phosphatase PP1-beta	38.0/6.08	37.5/6.03	23.9
156	P37140	PP1B_HUMAN	Serine/threonine protein phosphatase PP1-beta	38.0/6.08	38.1/6.13	24.5
Signaling molecule						
294	O43399	TD54_HUMAN	Tumor protein D54	22.3/5.11	30.6/5.32	45.1
220	P09382	LEG1_HUMAN	Galectin-1	14.9/5.23	11.3/4.89	73.9
244	P17931	LEG3_HUMAN	Galectin-3	26.3/9.12	30.3/8.64	28
268	Q15691	MAE1_HUMAN	Microtubule-associated protein RP/EB family member 1	30.2/4.86	33.3/5.17	26.9
Ion channel						
96	Q02641	CCB1_HUMAN	Voltage-dependent calcium channel beta-1b subunit	65.7/6.33	70.0/7.19	10.8
189	O00299	CLI1_HUMAN	Chloride intracellular channel protein 1	27.3/4.93	32.2/5.22	57.3
236	P45880	POR2_HUMAN	Voltage-dependent anion-selective channel protein 2	38.7/6.72	33.4/7.47	29.3
242	P21796	POR1_HUMAN	Voltage-dependent anion-selective channel protein 1	30.9/9.04	32.9/8.79	25.1
Ligase						
3	P22314	UBA1_HUMAN	Ubiquitin-activating enzyme E1	117.8/5.49	103.0/5.12	3.8
120	P00966	ASSY_HUMAN	Argininosuccinate synthase	46.7/8.33	46.2/8.06	25.2
200	P27924	UBC1_HUMAN	Ubiquitin-conjugating enzyme E2-25 kDa	22.5/5.21	27.5/5.30	19
Transcription factor						
85	Q9UQ80	P2G4_HUMAN	Proliferation-associated 2G4, 38 kD	43.8/6.13	51.3/6.32	12.5
89	P78381	UGAT_HUMAN	UDP-galactose translocator	41.3/9.98	54.7/6.38	11.8
Extracellular matrix						
43	P18206	VINC_HUMAN	Vinculin	117.3/5.51	110.1/6.21	8.4
44	P18206	VINC_HUMAN	Vinculin	117.3/5.51	110.1/6.26	8.4
Immunity and defense						
13	P11142	HS7C_HUMAN	Heat shock cognate 71 kDa protein	71.1/5.25	70.8/5.46	51.1
296	P11142	HS7C_HUMAN	Heat shock cognate 71 kDa protein	71.2/5.25	72.5/6.41	34.5
300	P11142	HS7C_HUMAN	Heat shock cognate 71 kDa protein	71.2/5.25	72.0/5.39	46.4
Transfer/carrier protein						
111	Q16851	UDP2_HUMAN	UTP-glucose-1-phosphate uridylyltransferase 2	57.1/7.69	54.4/7.73	18.1
226	Q01469	FABE_HUMAN	Fatty acid-binding protein, epidermal	15.5/6.96	13.5/6.35	39.3
Defense/immunity protein						
176	Q07021	MA32_HUMAN	Complement component 1, q subcomponent binding protein	31.3/4.74	33.2/3.98	13.2
Signal transduction						
278	P52888	MEPD_HUMAN	Thimet oligopeptidase	79.6/5.96	84.1/6.04	35.3
Nucleic acid						
243	P09651	ROA1_HUMAN	Heteogeneous nuclear ribonucleoprotein A1	39.0/10.06	33.6/9.13	45.0
312	Q93079	H2BJ_HUMAN	Histone H2B.j (H2B/j)	13.8/11.13	14.7/6.70	23.5
Phosphate						
17	P30153	2AAA_HUMAN	Serine/threonine protein phosphatase 2A	66.0/4.81	63.0/5.00	25.1
Receptor						
132	O96008	OM40_HUMAN	Probable mitochondrial import receptor subunit TOM40	38.2/7.25	41.6/7.43	18.0
Unknown						
4	P54814	SMOO_HUMAN	Smoothelin	99.0/8.65	103.1/5.7	8.6
9	Q14166	Y153_HUMAN	Hypothetical protein KIAA0153	74.5/5.4	86.2/5.42	11.8
14	Q13409	DY12_HUMAN	Dynein intermediate chain2, cytosolic	64.1/4.84	77.7/ 5.29	19.0
53	Q13228	SBP1_HUMAN	Selenium-binding protein 1	52.9/6.56	54.8/6.18	43.9
62	O60268	Y513_HUMAN	Hypothetical protein KIAA0513	46.6/4.98	50.1/5.14	12.4
63	O60664	TI47_HUMAN	Cargo selection protein TIP47	47.2/5.21	50.0/5.27	21.4
154	P37837	TAL1_HUMAN	Transaldolase	37.7/6.8	45.3/6.43	27.9
157	P37837	TAL1_HUMAN	Transaldolase	37.7/6.8	40.5/6.40	15.7
160	094760	DDH1_HUMAN	NG,NG-dimethylarginine dimethylaminohydlase 1	31.5/5.76	36.4/5.68	41.4
165	P50402	EMD_HUMAN	Emerin	29.1/5.25	39.1/4.59	34.6
169	P39149	ALU7_HUMAN	Alu subfamily SQ sequence contamination warning	54.4/11.29	69.0/3.98	23.0

Table 1 (*Continued*)

Spot no.[a]	Access. no.[b]	Swiss-prot name[c]	Protien description[d]	Theoretical[e] (Mr/p*I*)	Experimental[f] (Mr/p*I*)	Sequence[g] coverage (%)
199	P52565	GDIR_HUMAN	Rho GDP-dissociation inhibitor 1 (Rho GDI1)	23.3/4.85	28.0/5.05	48.0
205	P55957	BID_HUMAN	BH3 interacting domain death agonist;	22.0/5.27	25.6/5.40	7.0
206	13129100	ND	Hypothetical protein MGC5627	18.7/4.93	25.7/5.03	31.7
207	13129100	ND	Hypothetical protein MGC5627	18.7/4.93	25.7/5.03	31.7
217	7657176	ND	Transmembrane protein; putative typeII membrane	20.6/4.81	24.5/4.86	32.4
218	17462847	ND	Similar to putative	17.7/4.99	18.8/4.81	11.6
219	P47813	IF1A_HUMAN	Eukaryotic translation initiation factor 1A(EIF-1A)	16.4/4.92	12.7/4.90	54.5
221	47592121	ND	Beta-tubulin cofactor A	12.8/5.25	12.7/5.33	43.0
222	7705477	ND	Hypothetical protein	14.2/5.21	12.4/5.52	75.0
223	Q14259	ERH_HUMAN	Enhancer of rudimentary homolog	12.5/5.77	9.81/5.54	5.8
269	Q96C19	SWS_HUMAN	Swiprosin 1	26.8/4.97	33.0/5.04	29.6
297	Q12931	TRAL_HUMAN	Heat shock protein 75 kDa, mitochondrial precursor	80.3/8.12	75.4/6.52	25.7
310	D15509	AR20_HUMAN	APR2/3 complex 20 kDa subunit (P20-ARC)	19.8/8.65	20.0/8.65	21.4
45	18042949	ND	Unknown MGC: 17003	96.0/6.13	97.8/6.44	28.0
55	P31934	ROH1_HUMAN	Heterogeneous nuclear ribonucleoprotein H (hnRNP H)	49.5/6.26	53.3/6.08	48.6
60	Q12849	GRF1_HUMAN	G-rich sequenc factor-1 (GRSF-1)	48.5/5.59	55.2/5.25	12.1
64	P52597	ROF_HUMAN	Heterogeneous nuclear ribonucleoprotein F (hnRNP F)	46.0/5.39	49.4/5.43	26.3
79	P31943	ROH1_HUMAN	Heterogeneous nuclear ribonucleoprotein H (hnRNP H)	49.5/6.26	55.2/5.25	21.2
84	P35998	PRS7_HUMAN	26S protease regulatory subunit 7	49.0/5.73	51.3/5.97	29.6
113	P25705	ATPA_HUMAN	ATP synthase alpha chain, mitochondrial precursor	59.9/9.93	53.6/8.03	14.3
131	Q92524	PRSX_HUMAN	26S protease regulatory subunit S10B	44.4/7.49	44.7/7.39	25.4
146	P06748	NPM_HUMAN	Nucleophosmin (NPM)	32.7/4.47	38.9/5.42	29.3
147	Q03154	ACY1_HUMAN	Aminoacylase-1 (*N*-acyl-L-amino-acid amidohydrolase)	46.1/6.13	45.8/6.04	14.5
166	P13489	RINI_HUMAN	Placental ribonuclease inhibitor	51.8/4.54	51.2/4.95	19.9
167	Q09028	RB48_HUMAN	Chromatin assembly factor 1 P48 subunit	47.9/4.59	53.9/4.54	13.9
178	P31974	143S_HUMAN	14-3-3 protein sigma (Stratifin)	27.9/4.5	31.1/4.41	73.8
192	P35232	PHB_HUMAN	Prohibitin	29.9/5.55	31.2/5.60	59.9
196	P30040	ER29_HUMAN	Endoplasmic reticulum protein Erp29 precursor	29.1/7.46	29.9/5.90	33.7
201	Q9Y5S9	RBM8_HUMAN	RNA-binding protein 8	19.9/5.52	26.1/5.26	23.6
208	P30040	ER29_HUMAN	Endoplasmic reticulum protein Erp29 precursor	29.1/7.46	30.1/6.29	26.4
251	P30086	PEBP_HUMAN	Phosphatidylethanolamine-binding protein	20.9/7.43	26.0/7.74	7.9
258	P08206	S110_HUMAN	Calpactin I light chain (P11)	11.2/7.44	8.6/7.63	59.4
269	Q99426	TBCB_HUMAN	Tubulin-specific chaperone B (Tubulin folding cofactor)	27.6/4.89	33.0/5.04	29.9
276	P13798	ACPH_HUMAN	Acylamino-acid-releasing enzyme	82.3/5.25	90.0/5.41	20.1
289	P52272	ROM_HUMAN	Heterogeneous nuclear ribonucleoprotein M (hnRNP M)	77.6/9.35	75.8/8.65	33.3
290	P52272	ROM_HUMAN	Heterogeneous nuclear ribonucleoprotein M (hnRNP M)	77.6/9.35	74.7/8.78	33.3
291	P52272	ROM_HUMAN	Heterogeneous nuclear ribonucleoprotein M (hnRNP M)	77.6/9.35	74.8/8.88	33.3
303	P43686	PRS6_HUMAN	26S protease regulatory subunit 6B	47.5/4.94	51.4/5.20	31.6
303	P17980	PRSA_HUMAN	26S protease regulatory subunit 6A	49.4/4.92	51.4/5.20	60.8
197	P13693	TCTP_HUMAN	Translationally controlled tummo protein (TCTP)(P23)	19.7/4.67	27.1/4.77	39.0
186	095994	ND	Anterior gradient 2 homolog	20.0/9.03	16.5/8.99	9.9

[a]Spot numbers (spot nos.) correspond to those in Fig. 2. [b]Accession number, [c]Swiss-prot name, [d]protein description, [e]theoretical molecular weight and isoelectric point (theoretical Mr/p*I*), [f]observed molecular weight and isoelectric point (experimental Mr/p*I*) were obtained based on the location of the spots on the 2D gel. [g]The protein amino acid sequence coverage by the matching peptides (Sequence coverage (%)).

were compared (Fig. 3A and B, respectively). The overall differences were estimated by scatter plot analysis (Fig. 3C), showing that the intensity of 28.0% of the protein spots changed more than four-fold after treatment with phosphatase. Examples of the protein spots whose intensity was affected more than four-fold by phosphatase treatment are shown in Fig. 3D. As phosphorylation of a protein changes its p*I* and consequently its position in 2D gels, phosphatase treatment results in alterations of spot intensity. It is possible that some phosphorylated proteins might be resistant to phosphatase treatment and the number of phosphorylated proteins might be more than expected by this experiment. We considered that spots with decreased intensity after phosphatase treatment were probably phosphorylated in their original location on the 2D gel. On the other hand, we considered that spots with increased intensity after phosphatase treatment represent migration of the previously phosphorylated isoform to the location of the unphosphorylated isoform. The protein spots whose intensity was affected by phosphatase treatment are listed in Table 4. The proteins corresponding to these spots were identified by matching 2D iamge of experimental samples to the reference gel image (Fig. 2).

3.4. Application of the 2D database of Cy5-labeled proteins to colon cancer tissue

We compared the 2D profile of the colon cancer cell line DLD-1 with that of colon cancer cells obtained from surgical

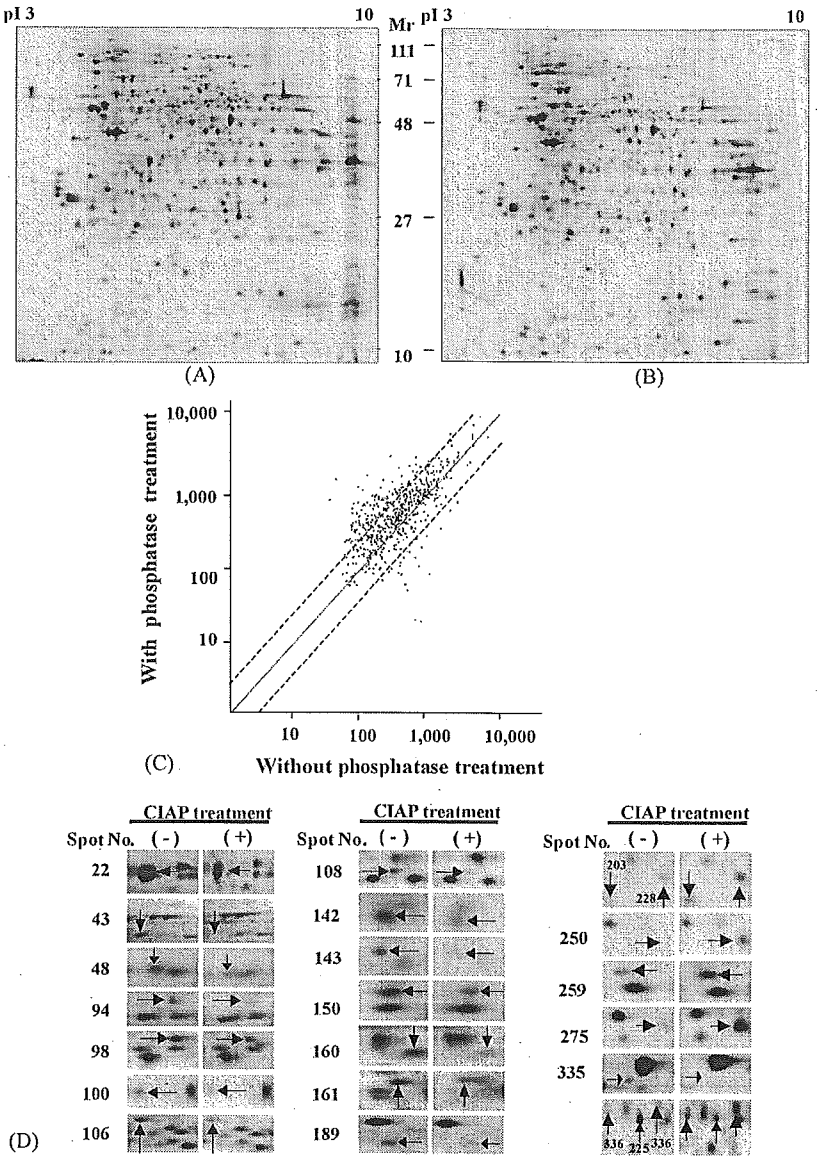

Fig. 3. Effects of phosphatase treatment on the intensity of the protein spots of DLD-1 cells. A protein lysate of DLD-1 cells was incubated with (A) and without (B) alkaline phosphatase, and the proteins were labeled with Cy3 and separated by 2D-PAGE. (C) The overall changes as a result of phosphatase exposure were estimated by scatter plot analysis with (x-axis) and without (y-axis) phosphatase exposure. The broken lines represent four-fold differences from the ($y = x$ axis). (D) The 2D images of the proteins with (+) and without (−) phosphatase are summarized. The arrows point to the protein spots whose intensity was changed more than four-fold by phosphatase treatment. The numbers correspond to those in Table 1, and the results are summarized in Table 4.

specimens by laser microdissection. Tissue sections were briefly stained with hematoxylin (Fig. 4A), and the cancer cells were isolated by laser microdissection (Fig. 4B). The overall 2D protein profiles of the DLD-1 cells (Fig. 4C) and the colon cancer cells (Fig. 4D) were compared by scatter plot analysis (Fig. 4E). To evaluate the similarity of these two 2D images, we performed the scatter plot analysis. Scatter plot analysis revealed that the intensity of 93% of the protein spots from the colon cancer cells was within four-fold of the intensity of the corresponding spots from DLD-1 cells. As most of the protein spots from the colon cancer cells were present on 2D image of DLD-1 cells, it could be possible to identify the proteins corresponding to the spots of colon cancer cells by matching the 2D image with the reference image in our database.

4. Discussion

We constructed a 2D database of fluorescence-labeled proteins of colon cancer cells. This is the first 2D database of fluorescence-labeled proteins of a higher eukaryotic proteome. Moreover, this is one of the largest databases of colon cancer cells, comprising 258 different gene products. To detect protein spots, we used currently developed fluorescent dye. The different detection methods may result in different

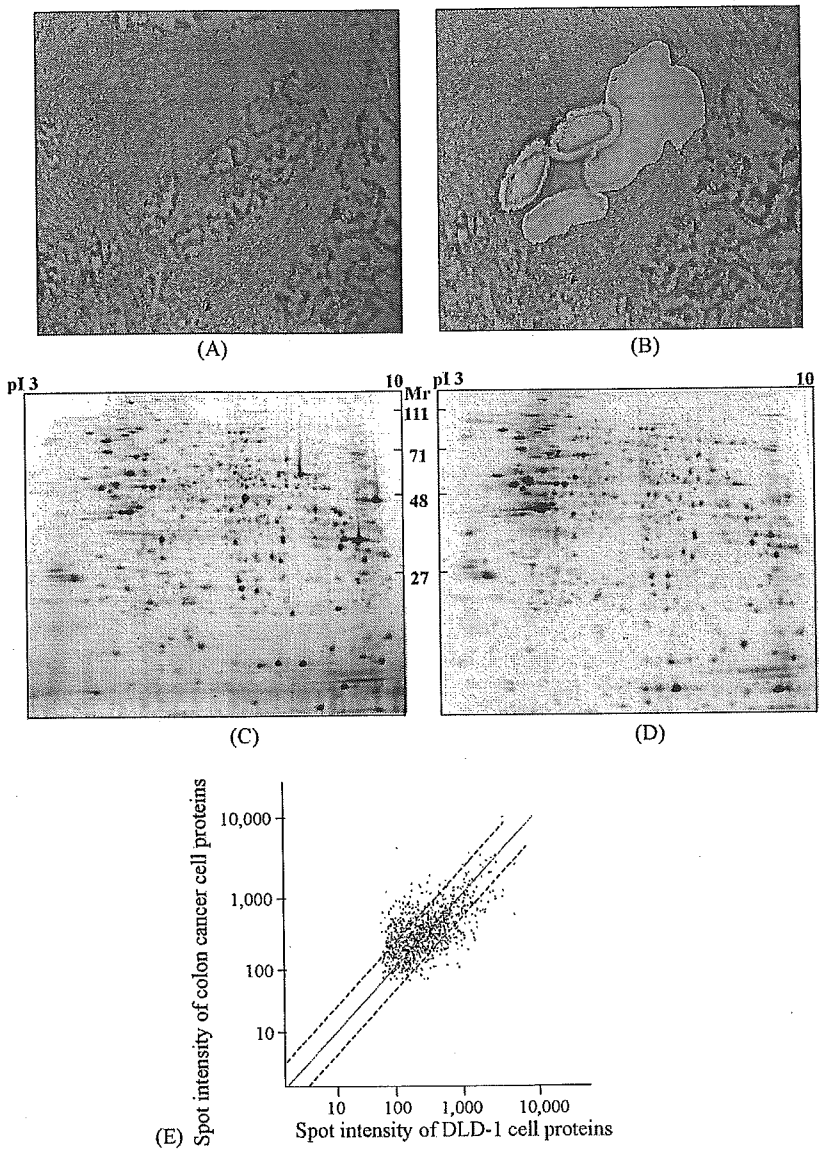

Fig. 4. Frozen colon cancer tissues were sectioned and stained with hematoxylin (A), and the tumor cells were recovered by laser microdissection (B). Overall comparison of the 2D profile of colon cancer cells (C) with that of DLD-1 cells (D). The coefficient was determined by scatter plot analysis. The broken lines represent four-fold differences from the ($y = x$ axis). The correlation coefficient (r) is 0.5.

2D images, due to the different specificities of the detection method. For example, the Cy5 fluorescent dye binds lysine residues of proteins [5], whereas SYPRO Ruby has strong affinity for lysine, arginine, and histidine residues and weak affinity for tyrosine and tryptophan residues [17]. Currently, several 2D databases for colon cancer cells [19–22] and a comparative proteomic study of colorectal carcinoma using 2D-PAGE [23–26] have been reported. We found that it was difficult to match the 2D images from these studies with the reference 2D image in our database, perhaps because of differences in protocols for protein extraction, electrophoresis and spot detection. However, because we used commercially available IPG gels and the results are highly reproducible, our database will be useful when an identical protocol is used to generate the 2D gel.

Functional classification of the identified proteins revealed that 42.5% of them could be categorized into the oxidoreductase, cytoskeletal protein, nucleic acid binding protein, chaperone, and isomerase families. Therefore, 2D-DIGE will be useful for studies focusing on these protein families, whereas proteins with lower expression levels will require more sensitive detection methods. We found that 52 proteins were represented by multiple spots. The total number of observed spots is approximately 1500 with our protocol. Consequently, assuming that the rate of spot redundancy, 258 proteins/314 spots, is similar for the rest of the protein spots, the total number of proteins in our database can be estimated as 1232. These results suggest that modified procedures will be required to enrich this small observed fraction of the proteome, because the total number of gene products

Table 2
Percentages of protein spots according to protein category

Protein category	Spots	Percentage (%)
Oxidoreductase	39	10.5
Cytoskeletal protein	35	9.4
Nucleic acid binding	33	8.9
Chaperone	26	7.0
Isomerase	25	6.7
Select calcium binding	22	5.9
Miscellaneous function	18	4.9
Select regulatory molecule	14	3.8
Transferase	14	3.8
Hydrolase	14	3.8
Protease	12	3.2
Kinase	11	3.0
Lyase	11	3.0
Synthase and synthetase	9	2.4
Cell adhesion molecule	6	1.6
Phosphatase	4	1.1
Signaling molecule	4	1.1
Ion channel	4	1.1
Ligase	3	0.8
Immunity and defense	3	0.8
Transcription factor	2	0.5
Extracellular matrix	2	0.5
Transfer/carrier protein	2	0.5
Nucleic acid	2	0.5
Defense/immunity protein	1	0.3
Signal transduction	1	0.3
Phosphate	1	0.3
Receptor	1	0.3
Unknown	52	14.0
Total	371	100.0

in any given cell is estimated to be around 10,000 and post-translational modifications of gene products should increase the total number of protein isoforms [27]. Fractionation and concentration of particular fractions of the proteome prior to electrophoresis [28], labeling of proteins with radioactivity [29], large format 2D gels [30] and combination of narrow-p*I* range IPG gels [31] can be used to increase the number of observable spots. To allow observation of a greater fraction of the proteome, there have also been intense efforts to develop mass spectrometry-based proteomic approaches complementary to 2D-PAGE. However, none of these technologies appears adequate to uncover the entire proteome, suggesting that a database for each approach will be required to understand its limitations, to avoid redundancy between the multiple methods and to integrate whole data.

Table 3
Proteins matching the same gene in Table 1

Name of protein	No. of isoforms detected
Heat shock cognate 71 kDa protein	5
Annexin II	5
Electron transfer flavoprotein alpha-subunit	4
Protein disulfide isomerase A3 precursor	4
Actin, cytoplasmic 1 (beta-actin)	3
Glyceraldehyde 3-phosphate dehydrogenase	3
Peptidyl-prolyl cis-trans isomerase A (PPIase)	3
Alpha enolase	3
Endoplasmin precursor (GRP94)	3
Heat shock protein HSP 90-alpha (HSP 86)	3
Isocit rate dehydrogenase (NADP) cytoplasmic	3
Eukaryotic translation initiation factor 3 subunit 2	3
Heterogeneous nuclear ribonucleoprotein M (hnRNP M)	3
Keratin, type I cytoskeletal 19 (CK19)	3
Serum albumin precursor	3
Ubiquinol-cytochrome C reductase complex core Protein I	3
Products of 36 different genes (2 spots for the same protein)	72

Summary of the spots identified that originated from the same genes. Of the 314 protein spots identified by mass spectrometry, 52 proteins appeared more than once. The names of the proteins are the same in Table 1.

Table 4
Phosphorylated proteins in Table 1

Spot no.	Protein name
22	60 kda heat shock protein
42	Alpha-1 catenin
95	Elongation factor 2 (EF2)
47	T-complex protein 1, alpha subunit
90	Seryl-trans synthetase
93	Stress induced-phosphoprotein 1
101	Glucose-6-phosphate 1-dehydrogenase (G6PD)
150	Annexin A7
160	Spermidine synthase
103	Elongation factor Tu, mitochondrial precurcer
306	Multifunctional protein ADE2
134	Aspartate aminotransferase, cytoplasmic
133	40 kDa peptidyl-proly cis-trans isomerase
141	60S acidic ribosomal protein P0
177	14-3-3 protein epsilon
229	Eukaryotic translation nitlation factor 4H
272	Esterase D
230	Electron transfer flavoprotein alpha subunit
307	Electron transfer flavoprotein alpha subunit
234	Phosphoglycerate mutase
250	Cofilin

The protein spots whose intensity changed more than four-fold were categorized as phosphorylated proteins. Spot number (spot no.) and protein names are the same as in Table 1.

To evaluate the phosphorylation status of our proteins, we examined the effects of phosphatase treatment on protein migration in the 2D gel. We found that the intensity of 28.0% of the spots was changed more than four-fold by phosphatase treatment. These results appear to differ from those of a recent study in which exposure of protein samples to phosphatase showed that 4.8% of the detectable proteins were phosphorylated [32]. We did not investigate whether this discrepancy was attributable to different conditions of phosphatase exposure or to differences between the proteome observed by fluorescent dye labeling and that observed by conventional colorimetric staining. It is also possible that the phosphorylation status of the proteome varies between different cells, since the previous study used cultured rat skin fibroblasts. Although more than 10% of proteins in a typical mammalian cell are thought to be phosphorylated, the exact number of phosphorylated proteins has not been determined. As the 2D-PAGE with phosphatase treated samples is conventional method to obtain the overview of phosphor-proteome, 2D-PAGE will be a useful tool for an initial step

for phospho-proteomics. Multiplex imaging using different dyes is a powerful tool to compare the samples before and after the treatment, as it can detect the small alterations before and after the treatment without gel-to-gel variations. On the other hand, we need to bare in mind that it is possible that the proteins with exactly same p*I* and MW to some protein might appear by phosphatase treatment. Therefore, other approaches, such as Western blotting with antibodies against phosphorylated proteins and metabolic labeling of the cells with isotopes [33], will be helpful to compliment to the experiment of phosphatase treatment for the phospho-proteome. Mass spectrometry-based approaches will be also effective in studying the phospho-proteome. Shu et al. used liquid chromatography–tandem mass spectrometry to identify 107 phosphorylated proteins in murine B lymphocytes [34]. Integration of the results of gel-based and mass spectrometry-based proteomic approaches will be required to understand the complex phospho-proteome. In the present study, we examined only the phosphorylation status of protein spots. However, the presence of redundant protein spots that were unaffected by phosphatase treatment suggests that post-translational modifications other than phosphorylation such as glycosylation may also contribute to redundancy.

A 2D database is a powerful tool for rapid identification of the proteins corresponding to observed protein spots. The protein corresponding to a spot of interest can be identified by matching the 2D image of the experimental sample with the reference image in the database. We demonstrated that the 2D image of DLD-1 cells was similar to that of colon cancer cells. Therefore, our 2D database will be useful to identify the majority of proteins of colon cancer cells in vivo and can be used for proteomic studies of colon cancer tissues. In many cases, because only a limited amount of clinical material is available, it may be difficult to obtain enough amount of sample such as 500 μg protein for protein identification, especially as a laser-microdissection is employed to obtain the tumor cells. In that case, we can run 2D-PAGE with small amount of protein such as 50 μg to create the protein expression profiles for analytical purpose and, to identify the protein corresponding to the interesting spots, we can match the image of analytical gels to that of the reference image in the database for protein identification. The similarity of 2D images of in vitro and in vivo cells will facilitate the functional study of proteins. When interesting protein spots are found in in vivo cells, we may be able to study what stimuli alter the expression level and posttranslational modifications of the protein spots using in vitro cells. Comparison between the in vitro and in vivo images of 2D-PAGE will allow such study for many proteins simultaneously without specific antibodies.

References

[1] A. Gorg, C. Obermaier, G. Boguth, A. Harder, B. Scgeibe, R. Wildgruber, W. Weiss, Electrophoresis 21 (2000) 1037.
[2] S.M. Hanash, Electrophoresis 21 (2000) 1202.
[3] J.E. Celis, P. Gromov, I. Gromova, J.M.A. Moreira, T. Cabezon, N. Ambartsumian, M. Grigorian, E. Lukanidin, P. Straten, P. Guldberg, J. Bartkova, J. Bartek, J. Lukas, C. Lukas, A. Lykkesfeldt, M. Jaattela, P. Roepstorff, L. Bolund, T. Orntoft, N. Brunner, J. Overgaard, K. Sandelin, M. Blichert-Toft, H. Mouridsen, F.E. Rank, Mol. Cell. Proteomics 2 (2003) 369.
[4] G. Chen, T.G. Gharib, H. Wang, C.C. Huang, R. Kuick, D.G. Thomas, K.A. Shedden, D.E. Misek, J.M. Taylor, T.J. Giordano, S.L. Kardia, M.D. Iannettoni, J. Yee, P.J. Hogg, M.B. Orringer, S.M. Hanash, D.G. Beer, Proc. Natl. Acad. Sci. U.S.A. 100 (2003) 13537.
[5] M. Unlu, M.E. Morgan, J.S. Minden, Electrophoresis 18 (1997) 2071.
[6] M. Unlu, Biochem. Soc. Trans. 27 (1999) 547.
[7] R. Tonge, J. Shaw, B. Middleton, R. Rowlinson, S. Rayner, J. Young, F. Pognan, E. Hawkins, I. Currie, M. Davison, Proteomics 1 (2001) 377.
[8] F. von Eggeling, A. Gawriljuk, W. Fiedler, G. Ernst, U. Claussen, J. Klose, I. Romer, Int. J. Mol. Med. 8 (2001) 373.
[9] S. Gharbi, P. Gaffney, A. Yang, M.J. Zvelebil, R. Cramer, M.D. Waterfield, J.F. Timms, Mol. Cell. Proteomics 1 (2002) 91.
[10] G. Zhou, H. Li, D. DeCamp, S. Chen, H. Shu, Y. Gong, M. Flaig, J.W. Gillespie, N. Hu, P.R. Taylor, M.R. Emmert-Buck, L.A. Liotta, E.F. Petricoin III, Y. Zhao, Mol. Cell. Proteomics 1 (2002) 117.
[11] M. Seike, T. Kondo, Y. Mori, A. Gemma, S. Kudoh, M. Sakamoto, T.S. Yamada, Hirohashi Cancer Res. 63 (2003) 4641.
[12] T.T. Toda, M. Sugimoto, J. Chromatogr. B Analyt. Technol. Biomed. Life Sci. 787 (2003) 197.
[13] U. Edvardsson, H.B. von Lowenhielm, O. Panfilov, A.C. Nystrom, F. Nilsson, B. Dahllof, Proteomics 3 (2003) 468.
[14] M. Fountoulakis, L. Suter, J. Chromatogr. B Analyt. Technol. Biomed. Life Sci. 782 (2002) 197.
[15] T. Kondo, M. Seike, Y. Mori, K. Fujii, T. Yamada, S. Hirohashi, Proteomics 3 (2003) 1758.
[16] A. Shevchenko, A. Loboda, W. Ens, B. Schraven, K.G. Standing, A. Shevchenko, Electrophoresis 22 (2001) 1194.
[17] J.X. Yan, R.A. Harry, C. Spibey, M.J. Dunn, Electrophoresis 21 (2000) 3657.
[18] D. Medjahed, G.W. Smythers, D.A. Powell, R.M. Stephens, P.F. Lemkin, D.J. Munroe, Proteomics 3 (2003) 129.
[19] G.E. Reid, H. Ji, J.S. Eddes, R.L. Moritz, R.J. Simpson, Electrophoresis 16 (1995) 1120.
[20] H. Ji, G.E. Reid, R.L. Moritz, J.S. Eddes, A.W. Burgess, R.J. Simpson, Electrophoresis 18 (1997) 605.
[21] M.A. Reymond, J.C. Sanchez, G.J. Hughes, K. Gunther, J. Riese, S. Tortola, M.A. Peinado, T. Kirchner, W. Hohenberger, D.F. Hochstrasser, F. Kockerling, Electrophoresis 18 (1997) 2842.
[22] R.J. Simpson, L.M. Connolly, J.S. Eddes, J.J. Pereira, R.L. Moritz, G.E. Reid, Electrophoresis 21 (2000) 1707.
[23] H. Ji, R.H. Whitehead, G.E. Reid, R.L. Moritz, L.D. Ward, R.J. Simpson, Electrophoresis 15 (1994) 391.
[24] J. Stulik, K. Koupilova, J. Osterreicher, J. Knizek, A. Macela, J. Bures, P. Jandik, F. Langr, K. Dedic, P.R. Jungblut, Electrophoresis 20 (1999) 3638.
[25] J. Stulik, J. Osterreicher, K. Koupilova, J. Knizek, J. Bures, P. Jandik, F. Langr, K. Dedic, B.W. Schafer, C.W. Heizmann, Eur. J. Cancer 36 (2000) 1050.
[26] L.C. Lawrie, S. Curran, H.L. McLeod, J.E. Fothergill, G.I. Murray, Mol. Pathol. 54 (2001) 253.
[27] L.A. Huber, Nat. Rev. Mol. Cell Biol. 4 (2003) 74.
[28] X. Zuo, D.W. Speicher, Anal. Biochem. 284 (2000) 266.
[29] J.A. Westbrook, J.X. Yan, R. Wait, M.J. Dunn, Proteomics 1 (2001) 370.

[30] J. Klose, C. Nock, M. Hermann, K. Stuhler, K. Marcus, M. Bluggel, E. Krause, L.C. Schalkwyk, S. Rastan, S.D. Brown, K. Bussow, H. Himmelbauer, H. Lehrach, Nat. Genet. 30 (2002) 385.
[31] J.A. Westbrook, J.X. Yan, R. Wait, S.Y. Welson, M.J. Dunn, Electrophoresis 22 (2001) 2865.
[32] A. Yamagata, D.B. Kristensen, Y. Takeda, Y. Miyamoto, K. Okada, M. Inamatsu, K. Yoshizato, Proteomics 2 (2002) 1267.
[33] A.K. Bendt, A. Burkovski, S. Schaffer, M. Bott, M. Farwick, T. Hermann, Proteomics 3 (2003) 1637.
[34] H. Shu, S. Chen, Q. Bi, M. Mumby, D.L. Brekken, Mol. Cell. Proteomics 3 (2004) 279.

Experimental Medicine
実験医学 月刊

別　刷

株式会社 羊土社

〒101-0052
東京都千代田区神田小川町2-5-1 神田三和ビル
TEL：03(5282)1215　FAX：03(5282)1212
E-mail：eigyo@yodosha.co.jp
URL：http://www.yodosha.co.jp/

プロテオミクスによる癌の悪性形質を裏付けるタンパク質群の同定

オーダーメイド医療のための腫瘍マーカーの開発へ向けた試み

近藤　格

プロテオミクスの分野では技術開発と並行して癌の網羅的タンパク質発現解析が盛んに行われている．臨床応用に最も近い研究例としてはオーダーメイド医療のための腫瘍マーカーの開発があげられる．癌の悪性形質を裏付けるタンパク質群をプロテオミクスの技術で同定し，より正確な診断を行い最適の治療法を選択するための腫瘍マーカーとして使用しようとする試みである．すでに肺癌や脳腫瘍に関しては癌患者の予後を予測できるタンパク質群がプロテオミクスの技術で報告されており，実用化へ向けた発展が期待される．

キーワード●　網羅的タンパク質発現解析，二次元電気泳動，予後，抗癌剤耐性

はじめに

プロテオミクスはinfancyな状態である，とよく語られる．タンパク質の全体像をとらえ，全体像をとらえることでしか得られない知見をもって生命現象を解明する，というプロテオミクス本来のアイデアからすれば，学問としてのプロテオミクスは確かにまだまだ完成度は低い．実際，プロテオミクスの分野で最もホットなトピックスは方法論に関するものであり，確立されて開発がプラトーに達した方法論は未だ存在しない．古典的といわれる二次元電気泳動ですら従来から指摘されていた弱点が克服されるブレークスルーが新しい蛍光試薬によってもたらされ，応用範囲が大きく広がった[1]．一方，派手な宣伝文句とともに登場した技術であっても実際に生物学的なデータを出すにあたって克服するべき問題点が明らかになっている技術もある．技術改良の傍らでは網羅的タンパク質発現解析が進みつつあり，その結果のフィードバックからそれぞれの技術の特性や限界について専門家の間では共通の認識が得られつつある．このような技術開発の時代はこれからもしばらく続くだろう．高額な機械を導入しさえすれば飛躍的に研究が進むとする非現実的な楽観論や，無数にあるタンパク質を包括的に理解することは到底できないとする極端な悲観論は影をひそめ，プロテオミクスの困難さが具体的なイメージを伴って理解されはじめているということが，プロテオミクスのここ数年の最大の進歩である．

癌研究における網羅的タンパク質発現解析は30年前に二次元電気泳動が発表されたころから行われている．ここ数年は最新のプロテオミクスの手法（ゲノムデータベースと質量分析の組合わせによる微量タンパク質の同定技術），いわゆるIT関連技術（大量のデータをネットワーク上で高速に扱う技術とデータマイニングの手法），そしてリファインされた古典的タンパク質分離技術（液体クロマトグラフィー，ゲル電気泳動など）などが組合わされ，従来の発現解析の限界を凌駕する応用が試みられている．癌研究におけるタンパク質発現解析のテーマも，従来は正常組織と癌組織を比較するという大雑把なものだったが，最近では特定の癌の形質に焦点を絞り，癌の複雑な悪性形質（不

Cancer proteomics for personalized medicine

Tadashi Kondo：Cancer Proteomics Project, National Cancer Center Research Institute（国立がんセンター研究所腫瘍プロテオミクスプロジェクト）